IC/IR/2001/17
INTERNAL REPORT
(Limited Distribution)

United Nations Educational Scientific and Cultural Organization
and
International Atomic Energy Agency
THE ABDUS SALAM INTERNATIONAL CENTRE FOR THEORETICAL PHYSICS

THEORY OF NOVEL NORMAL AND SUPERCONDUCTING STATES IN DOPED OXIDE HIGH-T_c SUPERCONDUCTORS

S. Dzhumanov
Institute of Nuclear Physics, Uzbek Academy of Sciences,
Ulugbek, Tashkent, 702132, Uzbekistan[1]
and
The Abdus Salam International Centre for Theoretical Physics, Trieste, Italy.

MIRAMARE – TRIESTE
October 2001

[1]Permanent address.

Abstract

A consistent and complete theory of the novel normal and superconducting (SC) states of doped high-T_c superconductors (HTSC) is developed by combining the continuum model of carrier self-trapping, the tight-binding model and the novel Fermi-Bose-liquid (FBL) model. The ground-state energy of carriers in lightly doped HTSC is calculated within the continuum model and adiabatic approximation using the variational method. The destruction of the long-range antiferromagnetic (AF) order at low doping $x \geq x_{c1} \simeq 0.015$, the formation of the in-gap states or bands and novel (bi)polaronic insulating phases at $x < x_{c2} \simeq 0.06 - 0.08$, and the new metal-insulator transition at $x \simeq x_{c2}$ in HTSC are studied within the continuum model of impurity (defect) centers and large (bi)polarons by using the appropriate tight-binding approximations. It is found that the three-dimensional (3d) large (bi)polarons are formed at $\varepsilon_\infty/\varepsilon_0 \leq 0.1$ and become itinerant when the (bi)polaronic insulator-to-(bi)polaronic metal transitions occur at $x = x_{c2}$. We show that the novel pseudogapped metallic and SC states in HTSC are formed at $x_{c2} \leq x \leq x_p \simeq 0.20 - 0.24$. We demonstrate that the large polaronic and small BCS-like pairing pseudogaps opening in the excitation spectrum of underdoped ($x_{c2} < x < x_{BCS} = 0.125$), optimally doped ($x_{BCS} < x < x_o \simeq 0.20$) and overdoped ($x > x_o$) HTSC above T_c are unrelated to superconductivity and they are responsible for the observed anomalous optical, transport, magnetic and other properties of these HTSC. We develop the original two-stage FBL model of novel superconductivity describing the combined novel BCS-like pairing scenario of fermions and true superfluid (SF) condensation scenario of composite bosons (i.e. bipolarons and cooperons) in any Fermi-systems, where the SF condensate gap Δ_B and the BCS-like pairing pseudogap Δ_F have different origins. The pair and single particle condensations of attracting 3d and two-dimensional (2d) composite bosons are responsible for the observed second- and first-order SC phase transitions in HTSC. We examine the relationship between the pairing pseudogap Δ_F and the SC gap Δ_B and their doping dependences. We argue that two distinct FBL scenarios of novel superconductivity are realized in so-called fermion superconductors (overdoped HTSC) and boson ones (underdoped and optimally doped HTSC). The formation of the stripe phases in underdoped HTSC is discussed within the large (bi)polaron model and the novel FBL model. It is shown that the novel normal and SC state properties of doped HTSC have not only 2d but also essentially 3d character. The generic and relevant electronic phase diagrams of doped HTSC are presented. The novel theory consistently and successfully explains existing experimental data.

1 Introduction

Since the discovery of high-T_c superconductivity by Bednortz and Muller [1], the normal and superconducting (SC) state properties of high-T_c superconductors (HTSC) have studied from the various points of view. Numerous experimental results indicate [2-16] that compared with conventional superconductors, the doped oxide HTSC seem to behave anomalously in the normal and SC states, especially in the underdoped and optimally doped regions. Understanding the nature of the anomalous (or novel) normal and SC state properties of doped copper and other oxides remains one of the central issues in condensed matter physics. Many theoretical studies devoted to this issue. These theoretical approaches are based mainly on the conventional band formalism and Mott-Hubbard models, (see [10,17,19-22]), different BCS-like s-, p- and d-wave pairing mechanisms (see [10,13,17,23], well-known Bose-Einstein condensation (BEC) models [17,24-27] and so-called resonating valence band (RVB) models [10,28,29]. So far current knowledge about the anomalous normal and SC state properties of doped oxide HTSC based on these theoretical model is limited enough (see also [11,12]). The insulating, metallic and SC states of these doped HTSC defy the conventional theories of insulators, metals and superconductors. In particular, fundamental problems such as the mechanisms responsible for the destruction of the long-range antiferromagnetic (AF) order [2,16], the formation of so-called in-gap states and bands [3,4,16,30], the doping and temperature-induced metal-insulator transitions (MIT's) [16,17], the formation of the stripes [31-34] and Bose (or spin) glass phases [2,16,17], the superconductor-insulator transition [35], the pseudogap formation and second-order SC phase transition (at $T = T_c$) [8,9,12,14,17,36-39], the first-order SC phase transition well below T_c [40-42], the non-zero density of states (DOS) inside and in the bottom of the assumed "SC" gap [37,43,44], the presence of two distinct pseudogaps in the excitation spectrum of underdoped and optimally doped HTSC [39,45,46] and the half-integer h/4e magnetic flux quantization [13] in doped HTSC remain complete mysteries to these theories. The evolution of the electronic structure of high-T_c cuprates from lightly doped insulator to underdoped metal or superconductor and then to ordinar metal in the overdoped regime raises key questions which are important pieces of the puzzle. For example, the relationship between the SC gap and the normal state pseudogap and their doping [18,37,38] and temperature [9,37] dependences are still unresolved. Further, most of the existing theoretical models are restricted to a two-dimensional (2d) case and to a rigid lattice approximation and the inherent three-dimensional (3d) properties [27,41] and the strong electron- phonon interactions [47] characteristic for HTSC are fully ignored. The solution of the above puzzling problems provides valuable insight into the anomalous normal and SC state properties of doped oxide HTSC. In particular, this provides a consistent picture of the microscopic origins of two pseudogaps and true SC gap and their crossover temperatures. In general, it is necessary for any theory to explain properly the existing anomalies not only above T_c, but also below T_c as well as a wealth of phenomena (e.g. transport, optical, magnetic

and other processes) and the remarkable doping and temperature dependences of the normal and SC state properties of HTSC.

In this paper an attempt has been made to develop the consistent and adequate quantitative theory of the novel normal and SC states of doped HTSC within the continuum model of real (r)-space (bi)polarons [48,49], the appropriate tight-binding models and the original two-stage Fermi-Bose-liquid (FBL) model of novel superconductivity [50,51]. First we discuss the insulating state of the undoped mother copper oxides in terms of the conventional Mott-Hubbard model and the Zaanen- Sawatzky-Allen classification scheme [17,20]. Then we discuss the possibility of the appearance of doped holes in the oxygen valence band and the restricted character of the conventional Mott-Hubbard model for description of the extended states of doped holes. Further, using the continuum model of the extrinsic and intrinsic carrier self-trapping [48,49,52], we find that the ground states of doped holes in polar compounds are the large- and nearly small-radius self-trapped (i.e. polaronic and bipolaronic) states. We show that the carriers in doped HTSC are basically large multisite (bi)polarons as earlier predicted in [25,53]. At low doping the (bi)polaronic states are formed in the charge-transfer (CT) gap of HTSC. We demonstrate that the increasing of the doping leads to the ionization of the hydrogen-like impurity (or defect) centers and then the immediate self-trapping of the liberated carriers in a deformable lattice leads to the formation of large and nearly small (bi)polarons. The appearance of (bi)polarons is responsible for the destruction of the long-range AF order and the formation of the novel (bi)polaronic insulating states in lightly doped HTSC. At higher doping we consider the formation possibility of the extrinsic in-gap Hubbard bands, the extrinsic and intrinsic in-gap (bi)polaronic bands within the appropriate tight-binding models. We show that the MIT in doped copper oxides and other polar systems is new (bi)polaron-induced MIT and not Mott transition as accepted now. The smooth MIT is responsible for the stripe formation in underdoped HTSC. Further, we study the pseudogap phenomena and their effects on the transport, optical, magnetic and other properties of the underdoped, optimally doped and overdoped HTSC on the basis of the novel FBL model [50,51]. We demonstrate that in the excitation spectrum of the underdoped and optimally doped HTSC the small BCS-like pairing pseudogap [50] and the large polaronic pseudogap [51] exist not only above T_c but also below T_c. This pseudogaps are unrelated to the SC gap. We argue that the novel superconductivity is driven by the superfluid (SF) condensations (i.e. single particle condensation (SPC) and pair condensation (PC)) of attracting composite bosons (Cooper pairs and bipolarons) but not by any pairing mechanisms of holes or electrons as accepted almost in all existing theories of superconductivity. The distinctive temperature dependences of the pairing pseudogap and the SC gap are discussed. The doping dependences of the two normal state crossover temperatures, SC transition temperature T_c, two pseudogaps and true SC gap are studied in detail. As a result, the complete and relevant temperature-doping phase diagrams of doped copper oxides are presented and their distinctive features are discussed. We demonstrate that the developed theory is in good agreement with

existing experimental results.

2 Electronic structure of undoped copper oxides

In undoped cuprates, the Cu^{2+} ion is surrounded by ligand oxygen ions O^{2-} with an octahedron configuration. The copper d state has fivefold degeneracy which is lifted by the cubic, tetragonal and orthorhombic crystal fields [17,20]. The low-lying t_{2g} and $d_{3z^2-r^2}$ states are fully occupied, whereas the highest $d_{x^2-y^2}$ state is half filled. Therefore, the single-band Hubbard model was choosen as the stating point for discription of the normal and SC state physics in high-T_c cuprates [10,17]. However, the another possible physical picture for copper oxides is the hibridization effect of the copper d orbitals and the oxygen p orbitals. In this case the copper d and the oxygen p orbitals form well separated bonding, non-bonding (NB) and antibonding (AB) bands and the Fermi level lies in the NB band [54]. The p-d model seems to be more suitable for description of the undoped copper oxides. The hamiltonian of the p-d model can be written as [17,20,54]

$$H = \varepsilon_d \sum_{i\sigma} d^+_{i\sigma} d_{i\sigma} + \varepsilon_p \sum_{j\sigma} + p^+_{j\sigma} p_{j\sigma} + t_{pd} \sum_{<ij>\sigma} d^+_{i\sigma} p_{j\sigma} +$$
$$+ U_d \sum_i n_{di\uparrow} n_{di\downarrow} + U_p \sum_j n_{pj\uparrow} n_{pj\downarrow} + V_{pd} \sum_{<ij>} n_{di} n_{pj}, \qquad (1)$$

where ε_d, ε_p and t_{pd} are the energies of the hole in the copper $d_{x^2-y^2}$ and oxygen p_σ orbitals and the hopping matrix element between Cu and O orbitals, respectively, U_d, U_p and V_{pd} are the energies of the Coulomb repulsion on Cu and O sites and the nearest-neighbor Coulomb repulsion between these sites, respectively, $d^+_{i\sigma}(d_{i\sigma})$ and $p^+_{j\sigma}(p_{j\sigma})$ are the d- and p-hole creation (annihilation) operators at the i-th and j-th sites, respectively with spin σ, $n_{di} = d^+_{i\sigma} d_{i\sigma}$ and $n_{pj} = p^+_{j\sigma} p_{j\sigma}$ are the number operators corresponding to the copper $d_{x^2-y^2}$ and oxygen p_σ orbitals, and $< ij >$ denotes the summation over all nearest-neighbor sites. The case $U_d = U_p = V_{pd} = 0$ (i.e. when there are no electron-electron correlations) corresponds to the conventional one-electron band structure and the valence band (i.e. AB band) is twofold degenerate, and therefore, is half-field. This degeneracy of the valence band is lifted by the strong Coulomb repulsion U_d with the formation of the lower filled and the upper empty Hubbard bands. Hamiltonian (1) shows that the electronic structure of the undoped transition metal oxides at $\varepsilon_p - \varepsilon_d = \Delta_{pd} > U_d$ corresponds to the Mott-Hubbard type insulators. While at $U_d > \Delta_{pd}$ the lower Hubbard band (LHB) lies below the oxygen p band. In such a case, the minimum CT excitation gap Δ_{CT} is formed between the upper Hubbard band (UHB) and fully occupied oxygen p band. According to the Zaanen-Sawatzky-Allen classification scheme [17,20,22] the undoped transition metal oxides at $U_d > \Delta_{pd}$ are called CT type insulators. Various experimental results show [20,22,55] that the resonable values of parameters are $U_d \simeq 10\,eV$, $U_p \simeq U_d/2 \simeq 5\,eV$, $t_{pd} \simeq 1.5\,eV$, $\Delta_{pd} \simeq 2-3\,eV$, $V_{pd} \simeq 2\,eV$. So, the undoped cuprates are typical CT insulators with the long-range AF order of copper d spins (d^9). We believe that the same single-band or three-band Hubbard models

describing the electronic structure of the undoped cuprates cannot be applied to the doped compounds in which the doped carriers can be delocalized just as in semiconductors (e.g. Si and Ge). For this reason, the adequate description of the electronic structure of doped cuprates and other oxides requires more reliable and realistic theoretical approaches.

3 Electronic structure of doped copper oxides

The ground state of doped carriers and the electronic structure of the doped polar compounds are still unresolved issues in condensed matter physics. In order to resolve these puzzling problems, we take $La_{2-x}Sr_xCuO_4$ (LSCO) as a typical doped oxide high-T_c superconductor. In the undoped parent compound the valence band is formed predominantly by oxygen p states with some admixture of copper d states, whereas the conduction band (i.e. UHB) is formed mainly by copper d states with some admixture of oxygen p states. This CT insulator can be doped with holes by substituting of impurity ions for host lattice ions or by excees oxygen atoms. As a result, the valence band of these compounds (e.g. LSCO and $YBa_2Cu_3O_{7-8}$ (YBCO)) is occupied by doped holes just as in doped semiconductors Si and Ge.

3.1 In-gap impurity states and bands

The doped holes are trapped by impurity (or defect) potentials and are localized first around the substitional ions or the oxygen vacancies (i.e. in YBCO). The stability of such an impurity (or a defect)-bound hole system in the phonon fields depends on the character of the hole-defect, defect-phonon and hole-phonon interactions [52]. Now we calculate the ground state energies of such an interacting system within the continuum model of extrinsic carrier self-trapping in doped HTSC. As is well known, in polar compounds both short- and long-range electron-phonon and defect-phonon interaction coexist. Then the total energies of the one-electron (hole) impurity center is given by the following functional [52]

$$E_1\{\psi,\Delta,\varphi\} = \int \psi(r)\left[-\frac{\hbar^2}{2m^*}\nabla^2 + V_{sD}\delta(r) - \frac{Ze}{\varepsilon_\infty r}\right]\psi(r)d^3r +$$
$$+\int\left[E_d\psi^2(r) + E_{dD}\delta(r)\right]\Delta(r)d^3r + \int\left[-e\psi^2(r) + Ze\delta(r)\right]\psi(r)d^3r + \frac{K}{2}\int\Delta^2(r)d^3r +$$
$$+\frac{\tilde{\varepsilon}}{8\pi}\int(\nabla\varphi(r))^2d^3r, \quad (2)$$

where $\psi(r)$ is the one-electron wave function, m^* is the effective mass of a carrier, V_{sD} is the short-range defect potential, Ze is the charge of a defect, ε_∞ is the high frequency dielectric constant, E_d and E_{dD} are deformation potentials of a carrier and a defect, respectively, $\Delta(r)$ and $\varphi(r)$ are the elastic dilation and electrostatic potential, respectively characterizing the lattice deformation and polarization, K is an elastic constant, $\tilde{\varepsilon} = \varepsilon_\infty/(1-\eta)$, $\eta = \varepsilon_\infty/\varepsilon_0$, ε_0 is the static dielectric constant.

The total energy of the two-electron (hole) impurity center can be calculated with and without inclusion of the interelectron correlation. First we ignore this correlation effect. Then the total energy of the two-carrier impurity center $E_2\{\Psi, \Delta, \varphi\}$ is given by simple doubling the terms with $\psi^2(r)$ in $Eq.(2)$ and adding the Coulomb repulsion energy

$$\int\int \psi^2(r_1)\frac{e^2}{\varepsilon_\infty|r_1 - r_2|}\psi^2(r_2)d^3r_1 d^3r_2, \tag{3}$$

where $\Psi(r_1, r_2)$ is the two-electron wave function approximated by a product $\psi(r_1)\psi(r_2)$. Minimization of the functionals $E_1\{\psi, \Delta, \varphi\}$ and $E_2\{\Psi, \Delta, \varphi\}$ first with respect to $\Delta(r)$ and $\varphi(r)$ and then with respect to a trial wave function choosen in the simple form [52]

$$\psi(r) = (\alpha\sqrt{2}/a_0)^{3/2}exp[-\pi(\alpha r/a_0)^2], \tag{4}$$

gives the following functionals

$$E_1(\alpha) = B[\alpha^2 - g_s\alpha^3 - g_l\alpha] \tag{5}$$

and

$$E_2(\alpha) = 2B[\alpha^2 - G_s\alpha^3 - G_l\alpha], \tag{6}$$

where $B = 3\pi\hbar^2/2m^*a_0^2$, $g_s = g_{SL}(1 + b_s)$, $g_l = g_{lL}(1 - \eta + \eta b_l)$, $G_s = g_{SL}(2 + b_s)$, $G_l = g_{lL}(1 - 2\eta + \eta b_l)$, $g_{SL} = E_d^2/2Ka_0^2B$, $g_{lL} = e^2/\varepsilon_\infty a_0 B$, $b_s = 2^{5/2}[(E_{dD}/E_d) - (KV_{sD}/E_d^2]$, $b_l = 2^{2/3}Z$, α is the variational parameter characterizing the localization degree of a carrier, a_0 is the lattice constant.

The functionals (5) and (6) have the minimums at $\alpha = \alpha_D = [1 - \sqrt{1 - 3g_sg_l}]/3g_s < 1$ and $\alpha = \alpha_D = [1 - \sqrt{1 - 3G_sG_l}]/3G_s < 1$, respectively. These minimums of the functionals (5) and (6) corresponding to the formation of large-radius $a_D > a_0$ delocalized (D) impurity (defect) states are determined from the relations [56]

$$E_1(\alpha_D) = \frac{B}{27g_s^2}\left[2 - 9g_sg_l - 2(1 - 3g_sg_l)^{3/2}\right] \tag{7}$$

and

$$E_2(\alpha_D) = \frac{2B}{27G_s^2}\left[2 - 9G_sG_l - 2(1 - 3G_sG_l)^{3/2}\right], \tag{8}$$

respectively.

The functionals (5) and (6) may have other minimums at $\alpha = \alpha_L \simeq 1$ corresponding to the formation of the nearly small-radius $a_L \simeq a_0$ localized (L) impurity states. It should be noted that the contribution of the long-range screening potential $Ze^2/\tilde{\varepsilon}r$ in (2) reduces the impurity Coulomb potential -$Ze^2/\varepsilon_\infty r$ into -$Ze^2/\varepsilon_0 r$ (see [25,52]).

Now we take into account the intercarrier correlation. After minimization of the functionals $E_1\{\psi, \Delta, \varphi\}$ and $E_2\{\Psi, \Delta, \varphi\}$ with respect to Δ and φ we obtain the functional depending on ψ and Ψ. We choose the trial wave function Ψ in the form

$$\Psi(r_1, r_2) = N[1 + \beta(\sigma r_{12})^2]exp\{-\sigma^2(r_1^2 + r_2^2)\}, \tag{9}$$

where β and σ the variational parameters, $N = (\sqrt{2}\alpha/a_0)^3/\sqrt{C_1(\beta)}$, $C_1(\beta) = 1 + 3\beta + 15\beta^2/4$, $\sigma^2 = \pi\alpha^2/a_0^2$, r_{12} is the relative distance between the carriers which have the coordinates r_1 and r_2.

Calculation of the integrals in the obtained functional $E_2\{\Psi\}$ gives

$$E_2(\alpha,\beta) = 2B\frac{C_2(\beta)}{C_1(\beta)}\left[\alpha^2 - C_s(\beta)\alpha^3 - G_l(\beta)\alpha\right], \tag{10}$$

where

$$G_s(\beta) = g_{sL}\left[\frac{2C_3(\beta)}{C_1(\beta)C_2(\beta)} + \frac{b_s C_1(\beta)}{C_2(\beta)}\right],\ G_l(\beta) = g_{lL}\left[\frac{C_5(\beta)}{C_1(\beta)C_2(\beta)} + \frac{b_l\eta C_6(\beta)}{C_2(\beta)} - \frac{2\eta C_7(\beta)}{C_1(\beta)C_2(\beta)}\right],$$

$C_2(\beta) = 1 + 2\beta + 13\beta^2/4$, $C_3(\beta) = 1 + (9/2)\beta + (309/32)\beta^2 + (1395/128)\beta^3 + (23745/4096)\beta^4$, $C_4(\beta) = 1 + (3/2)\beta + (15/16)\beta^2$, $C_5(\beta) = 1 + 6\beta + (261/16)\beta^2 + (1437/64)\beta^3 + (28185/2048)\beta^4$, $C_6(\beta) = 1 + 5\beta + (35/4)\beta^2$, $C_7(\beta) = 1 + (11/2)\beta + (449/32)\beta^2 + (2301/128)\beta^3 + (43545/4096)\beta^4$.

The conditions for the formation of the stable D and metastable L or stable L and metastable D states of one- and two-carrier impurity centers are defined as $E_1(\alpha_D) < E_1(\alpha_L)$, $E_2(\alpha_D) < E_2(\alpha_L)$ and $E_1(\alpha_D) > E_1(\alpha_L)$, $E_2(\alpha_D) > E_2(\alpha_L)$, respectively. At $b_s < 0$ (i.e. $E_{dD} < 0$) the short-range impurity potential is repulsive and it can be considered like a hard core (see also [52]). In this case the carrier-phonon interactions around the impurity ion (e.g. Sr^{2+} in LSCO) or defect (i.e. oxygen vacancy in YBCO) are suppressed by the short-range repulsive defect potential. Therefore, at $b_s < 0$ a rigid lattice model is a good approximation and the impurity states can be described properly by the hydrogen-like model [51]. In particular, in LSCO the substitutional impurity ion Sr^{2+} with radius larger than the host ion La^{3+} [2] has negative E_{dD} [52] and the situation $b_s < 0$ is realized. While the sign of the E_{dD} is not definite for a vacancy. Apparently, the oxygen vacancy in YBCO and other oxide HTSC has also negative E_{dD}. So, at $b_s < 0$ using the simple hydrogen-like model for description of the acceptor centers and in-gap impurity states in doped HTSC is well justified. Then in the lightly doped HTSC the in-gap impurity bands are formed as the extrinsic lower and Hubbard bands. The ionization energy E_I and the Bohr radius a_H of the localized impurity states are given by

$$E_I \simeq 13.6\left(\frac{Z}{\varepsilon_{eff}}\right)^2\frac{m^*}{m_e}\ eV \tag{11}$$

and

$$a_H = 0.53\frac{\varepsilon_{eff}}{Z}\frac{m_e}{m^*}\ A, \tag{12}$$

where ε_{eff} is the effective dielectric constant.

The hydrogenic impurity centers can form a simple superlattice with lattice constant a and long-range AF order [51]. If the half bandwidth of the impurity band $W_I/2 = Jf(z)$ determined in terms of the tight-binding model exceeds E_I, the half-filled impurity band merges with the valence band and the ionization of impurity centers occurs, where $J = \hbar^2/2m^*a^2$ is the transfer energy of the tight-binding model, $f(z)$ is any function which can be approximated as $f(z) = z$,

z is the coordination number (for cubic lattice $z = 6$). For Sr^{2+} ion in LSCO and oxygen vacancy in YBCO, we can assume $Z = 1$ and $Z = 1.5$, respectively. The band mass of carriers in HTSC is about $m^* \simeq (1.4 - 2.0)m_e$ [16,57] and we take $m^* \simeq 1.5m_e$. We believe that the simple approximation $\varepsilon_{eff} \simeq (5 - 7)\varepsilon_\infty$ is more suitable for doped cuprates with $\eta << 1$ (e.g. $\varepsilon_\infty = 2 - 7$ [2,25,58] and $\varepsilon_0 = 22 - 105$ [16,25,57-59]). For other oxides (i.e. NiO, TiO_2 and $SrTiO_3$) different approximations are discussed (see [60]), but these approximations are unserviceable for oxide HTSC. So, assuming $\varepsilon_\infty \simeq 5$ and $\varepsilon_{eff} = 5\varepsilon_\infty$ we obtain $E_I \simeq 0.032eV$ and $a_H = 8.3A$ for the Sr acceptor in LSCO. For YBCO the relation $\varepsilon_{eff} \simeq 7\varepsilon_\infty$ seems to be reasonable approximation and assuming $\varepsilon_\infty = 4.5$ [2] we find $E_I \simeq 0.045eV$ and $a_H \simeq 7.4A$. The above presented values of E_I and a_H are close to the observed values of $E_I \simeq 0.02 - 0.035eV$ and $a_H \simeq 8A$ for acceptor centers in HTSC [16]. While the values of the critical doping concentration $x_{c1} = n_{c1}/n_a \simeq 0.014$ in LSCO calculated by using the relation $Jf(z) = E_I$ is also close to the observed doping value $x_{c1} = 0.02$ [2,16,17] for destruction of the AF order, where $n_{c1} = 1/V_I$ and $n_a = 1/V_a$, $V_I = a^3 \simeq 10^4A^3$ is the volume per one impurity center, $V_a = 137A^3$ is the volume per CuO_2 unit in the orthorhombic LSCO.

Now the question, whether a MIT for a Hubbard model exists -an unresolved problem. Here we show the irrelevance of the Mott transition to the MIT and to the destruction of the AF order in doped cuprates. In the lightly doped HTSC the hydrogenic impurity states form the extrinsic lower and upper Hubbard bands in the CT gap. In such systems the acceptors give rise to an impurity band very close in energy to the valence band. In some infrared spectra the in-gap states have two components, one with finite energy and one almost with zero energy (see [61]). The latter can be assigned to the above impurity states, whereas the former should be attributed to the (bi)polaronic states (see below). In order to determine the energy gap between the extrinsic Hubbard bands, we calculate the Coulomb repulsive energy U between two carriers with antiparallel spins on the same impurity center using the variational method. The screening effects due to the presence of two carriers on the same impurity center lead to the decreasing of the total charge of this impurity. For this reason, we can assume that the two-carrier hydrogenic impurity has any effective or incomplete charge Z^*. The ground state energy of such an impurity $E_2(Z^*)$ depends on Z^*. Here we omit the standard variational calculation of the $E_2(Z^*)$ and present the final result:

$$E_2(Z^*) = Z^*(Z^* - 2Z + 5/8)\frac{e^2}{\varepsilon_{eff}a_H}. \tag{13}$$

Minimizing $E_2(Z^*)$ with respect to Z^* gives $Z^* = Z - 5/16$. Then the Mott-Hubbard gap is given by

$$U = \int\int \psi_{1s}^2(r_1)\frac{e^2}{\varepsilon_{eff}r_{12}}\psi_{1s}^2(r_2)d^3r_1d^3r_2 = \frac{10}{8}Z^*E_I, \tag{14}$$

where $E_I = e^2/2\varepsilon_{eff}a_H$, $\psi_{1s}(r) = 1/\sqrt{\pi}(Z^*/a_H)^{3/2}exp(-Z^*/a_H)$.

At $Z = 1$ we obtain $U \simeq 0.86E_I$. The proper criterion for Mott transition should be

determined from the relation

$$E_I = U \simeq 0.86E_I \text{ or } \frac{z\hbar^2}{m^*a^2} \simeq 0.86E_I, \tag{15}$$

from which, we obtain the following criterion for Mott transition

$$n_c^{1/3}a_H \simeq \sqrt{0.43/z}. \tag{16}$$

At $z = 6$ we find

$$n_c^{1/3}a_H \simeq 0.27. \tag{17}$$

The same criterion was also obtained in [62] within the another approach. At $a_H \simeq 8A$ the critical doping concentration x_m in LSCO calculated from the Mott criterion (17) is about $x_m \simeq 0.0055$ which is much lower than the above value $x_c = 0.02$. It means that the Mott transition in doped cuprates is unrelated to the destruction of the AF order and to the MIT which occurs at more higher doping level $x_c \simeq 0.05 - 0.07$ [2,16,17,32]. It is believed [51] that at $b_s < 0$ the MIT in doped cuprates is intrinsic (bi)polaronic MIT.

3.2 In-gap (bi)polaronic states and bands

At $W_I = U$ (or $x = x_m = 0.0055$) the upper and lower (singly-occupied) Hubbard bands would merge and they form the doubly-occupied half-filled ordinary band with half-bandwidth $W_I/(2) \simeq 0.43E_I$. So, the energy gap between this half-filled impurity band and valence band or the ionization energy of the acceptor is about $E_I - W_I/2 = 0.57E_I$. Further, with increasing doping level x up to $x_{c1} \sim 0.02$, the minimum ionization energy of the impurity center decreases and becomes zero when the half-filled impurity band merges with the valence band. At $x > x_{c1}$ the liberated carriers are immediately self-trapped in a deformable lattice between the impurity sites due to the strong short- and long-range electron-lattice interactions. The electron-lattice interactions in doped HTSC lead to the formation of large D and nearly small L (bi)polarons. Several theoretical approaches to the problem of a large D (bi)polaron in HTSC have been proposed so far [25,48,49,57], but there are no sufficient quantitative calculations (some numerical calculations for the tetragonal phase of HTSC are carried out in [48]) for HTSC. Now we calculate the formation possiblity of the large D (bi)polarons in doped 3d cuprates. In order to find the ground state energy of the interacting electron-lattice system, in (5), (6) and (10) we assume $b_s = 0$ and $Z = 0$. Then we obtain the following functionals of the total energies of polarons and bipolarons (with and without intercarrier correlation)

$$E_p(\alpha) = B[\alpha^2 - g_s\alpha^3 - g_l\alpha] \tag{18}$$

$$E_B(\alpha) = 2B[\alpha^2 - G_s\alpha^3 - G_l\alpha] \text{ with } \beta = 0 \tag{19}$$

and

$$E_B(\alpha) = 2B\frac{C_2(\beta)}{C_1(\beta)}\left[\alpha^2 - G_s(\beta)\alpha^3 - G_l(\beta)\alpha\right] \text{ with } \beta \neq 0 \tag{20}$$

where $g_s = g_{sL}$, $g_l = g_{lL}(1-\eta)$, $G_s = 2g_{sL}$, $G_l = g_{lL}(1-2\eta)$,

$$G_s(\beta) = \frac{2g_{sL}C_3(\beta)}{C_1(\beta)C_2(\beta)},\ G_l(\beta) = g_{lL}\left[\frac{C_5(\beta)}{C_1(\beta)C_2(\beta)} - \frac{2\eta C_7(\beta)}{C_1(\beta)C_2(\beta)}\right].$$

The conditions for the formation of the large D polaron and bipolaron can be written in the forms

$$E_B(\alpha_D) - 2E_p(\alpha_D) > 0, \tag{21}$$

and

$$E_B(\alpha_D) - 2E_p(\alpha_D) < 0, \tag{22}$$

respectively.

The binding energies of large D polarons and bipolarons and the energy of large bipolarons are defined as $E_p(D) = |E_p(\alpha_D)|$ and $E_{bB}(D) = |E_B(\alpha_D) - 2E_p(\alpha_D)|$ and $E_B(D) = |E_B(\alpha_D)|$, respectively. Another characteristic parameter of the (bi)polaron theory is the ratio $R_{bB}(D) = E_{bB}(D)/2E_p(D)$. Here we demonstrate the formation possibility of large D (bi)polarons in the orthorhombic cuprates, where the $Cu^{2+} - O^{2-} - Cu^{2+}$ bond length along c-axis can be choosen as the lattice constant. So, we can take $a_0 \simeq 6A$, $m^* \simeq 1.5m_e$ [57], $\varepsilon_\infty = 5$ [2,16,25]. According to the spectroscopic data the bandwidth of the valence band of these compounds or the Fermi energy is about $E_F \simeq 7eV$ [63-65]. The value of E_d is estimated as $E_d = (2/3)E_F \simeq 4.666eV$. Then at $K \simeq 1.4 \cdot 10^{12} dyn/cm^2$ [2,66] we obtain $B \simeq 0.666eV$, $g_s = 0.0865$, $g_l = 0.72(1-\eta)$, $G_s = 0.173$ and $G_l = 0.72(1-2\eta)$. The values of η characteristic for cuprates are $\eta \simeq 0.01 - 0.1$. Our calculations show that in doped cuprates the formation of a 3d- large D bipolaron without electron correlation is possible only for $\eta < 0.01$. While, the formation of such a bipolaron with electron correlation is possible for $\eta \leq 0.1$ (see Table 1). However, the formation of a small L polaron and bipolaron in doped 3d orthorhombic cuprates is impossible. As the D and L states of 3d- (bi)polarons in these compounds are separated by very high potential barrier. In a 2d electronic system, there is no potential barrier between the D and L states of (bi)polarons (see also [25]). Therefore, in doped orthorhombic cuprates the formation of a small L (bi)polaron is possible in the CuO_2 layer.

If in any polar compound the value of g_s much larger than 0.1, the formation of a large D bipolaron becomes possible in the range $0 < \eta \leq \eta_c = 0.193$ [49]. The formation of a large D bipolaron in a wide range is possible only in a 2d electronic system [67]. The scaling relation between the ground state energies of 2d and 3d bipolarons has the form [68]

$$E_{2B}(\alpha_D) = \frac{2}{3}(\frac{3\pi}{4})^2 E_{3B}(\alpha_D). \tag{23}$$

According to [68] the formation of a large Pekar's bipolaron (at $g_s = 0$) in a 3d electronic system is possible for $\eta \leq \eta_c = 0.31$. However, this result disagrees with other theoretical results $\eta_c = 0.125 - 0.140$ (at $g_s = 0$) [45,49,57].

Table 1: The calculated values of the parameters of large 3d (bi)polarons with electron correlation in doped orthorhombic cuprates.

η	$E_p(D)eV$	$E_B(D)eV$	E_{bB}	R_{bB}
0.00	0.08942	0.22398	0.04515	0.25249
0.02	0.08581	0.20862	0.03699	0.21555
0.04	0.08229	0.19397	0.02939	0.17860
0.06	0.07884	0.17991	0.02223	0.14099
0.08	0.07547	0.16654	0.01560	0.10332
0.10	0.07217	0.15370	0.00935	0.06479

Now there is serious problem in describing excitations in lightly doped cuprates [2,16,17]. If the insulating state of these materials is considered as the state of the Mott insulator with the AF ordering, then it is difficult to describe the insulating behavior of lightly doped cuprates above the Neel temperature T_N [2,16,17]. The puzzling insulating state of lightly doped cuprates above T_N can be understood properly on the basis of the above theory of large (bi)polarons. As x is increased, the ionization of the hydrogenic impurity centers occurs and the formation of polarons and bipolarons leads to the destruction of the long-range AF order. We believe that the value of T_N can be estimated as $T_N \simeq E_I/k_B$ (where k_B is the Boltzmann constant). The above presented results show that the ionization energies of the hydrogenic impurity centers in LSCO and YBCO are about $E_I \simeq 0.03eV$ and $\simeq 0.045eV$, respectively. Therefore, we obtain $T_N \simeq E_I/k_B \simeq 350K$ and $T_N \simeq 522K$ for LSCO and YBCO, respectively. These values of T_N are consistent with the experimental values of $T_N \simeq (300-325)K$ and $\simeq 500K$ observed in LSCO and YBCO, respectively [2,16]. The characteristic energies of large D (bi)polarons $E_p(D)$, $E_B(D)$ and $E_{bB}(D)$ should be manifested in optical absorption spectra of doped HTSC. Indeed, the values of $E_{bB}(D)$ (see Table 1) are close to the observed energy gaps $\simeq 0.03-0.05eV$ in the electronic spectra of HTSC [2,5,8,9,14-16,36,69,70]. These values of $E_{bB}(D)$ correspond also to the absorption peaks of the far-infrared transmission spectra observed at $0.013-0.039eV$ in YBCO [70]. While, the values of $E_p(D) \simeq 0.1eV$ and $E_B(D) \simeq 0.2eV$ are consistent with the energies of the in-gap states observed in doped cuprates at $\simeq 0.1-0.2eV$ [2,16,45,71]. Other in-gap states observed in many oxide HTSC at $\simeq 0.5-0.7eV$ [2,15,16] can be ascribed to the energy levels of large D bipolarons which are formed in the 2d CuO_2 layer. As can be seen from (23) the localized in-gap states of these bipolarons (at $g_s = 0$) are expected to be much (nearly four times) deeper than such states of the large D bipolarons in a 3d electronic system.

Now we consider the (bi)polaron-induced MIT. We assume that the polarons just as impurity centers form any superlattice with the lattice constant a_p. In the case $E_B(\alpha_D) < 2E_p(\alpha_D)$ a large D bipolaron can exist and be energetically stable with respect to two separate large D polarons. If $E_B(\alpha_D) > 2E_p(\alpha_D)$ a large D bipolaron is energetically unstable with respect to decomposition into two separate large polarons. In this case the overlapping of the doubly-occupied half-filled polaronic band with valence band leads to the new MIT. As the carriers

density increases, first the carriers occupy the low energy bound states or polaronic states. As soon as all these states were filled at $n = n_{c2}$ (or $x = x_{c2}$), the carriers start to occupy the itinerant states and the transition of the system from the insulating phase to the metallic phase occurs. So, the dissociation of large D bipolarons and the subsequent overlapping of the douply-occupied half-filled polaronic band with the valence band lead to the (bi)polaronic MIT. In other words, the MIT driven by the strong electron-phonon interactions (or carrier localization) is possible when the kinetic energy of polarons exceeds their binding energy $E_p(D)$. We assume that the polarons form any superlattice and the bandwidth of the polaronic band can be determined within the tight-binding approximation. Then the criterion for the new (bi)polaronic MIT is defined as

$$Jf(z) = E_p(D) \tag{24}$$

or at $f(z) = z = 6$ this criterion can be written as

$$\frac{3\hbar^2}{m_p^* a_p^2} = E_p(D), \tag{25}$$

from which we find the critical doping value

$$n_{c2} = \frac{1}{V_p} = a_p^{-3} = (m_p^* E_p(D)/3\hbar^2)^{3/2}, \tag{26}$$

where m_p^* is the effective mass of a large D polaron. The calculated values of n_{c2} and $x_{c2} = n_c/n_a$ by using the values of $n_a = 7.3 \cdot 10^{21} cm^{-3}$, $m_p^* \simeq 2m_e$ [16] and $E_p(D)$ for different η are presented in Table 2.

4 Novel pseudogapped normal state

The origin of the anomalous metallic state of high-T_c cuprates is still controversial. The underdoped ($x_{c2} < x < x_o$), optimally doped ($x = x_o$) and even some overdoped ($x > x_o$) HTSC above the SC transition temperature T_c show various anomalous transport, magnetic, optical and other properties which are far from the conventional Fermi-liquid behaviors, especially in the underdoped and optimally doped regimes. One of such anomalous properties of hole-doped HTSC is the linear temperature dependence of the resistivity ρ observed above a certain lower crossover temperature $T^* > T_c$ in contrast to the T^2 law expected in the conventional Fermi-liquid. This T-linear behavior of the resistivity is not yet fully understood. The downward deviation of the resistivity from T-linear behavior observed below T^* in the underdoped and optimally doped HTSC [17,72,73] is another intriguing aspect. The magnetic susceptibility χ and the electronic entropy S_e these HTSC start to decrease below a certain upper crossover temperature T_0 [12,39]. Further, χ and S_e decrease more sharply as the temperature is lowered below T^*. In some overdoped HTSC the resistivity shows the normal metallic (i.e. T^2-low) behavior (see [73]. The above anomalous normal state properties of underdoped and optimally doped HTSC are discussed now in terms of the different pseudogap models [17,45,46]. The existence

Table 2: The critical doping concentrations for (bi)polaronic MIT in orthorhombic high-T_c cuprates at different η.

η	0.00	0.02	0.04	0.06	0.08	0.10
n_c 10^{21}cm^{-3}	0.689	0.645	0.608	0.570	0.536	0.500
x_{c2}	0.065	0.068	0.073	0.078	0.083	0.088

of a normal state pseudogap in HTSC were originally predicted as the spin-gap [10,74-76], the AF pseudogap [46,77], the phase fluctuations of the SC order parameter or the SC pairing pseudogap intimately related to the SC gap [78-80] and the novel fluctuationless BCS-like (or non - SC) pairing pseudogap unrelated to the SC gap [50,51,53]. The BEC-BCS crossover picture [27] is identical to the SC phase fluctuation scenario. By now very extensive and contradictory literature has developed on this subject. In the last years two distinctive pseudogaps opening in the excitation spectrum of underdoped and optimally doped HTSC at different crossover temperatures well above T_c are also discussed [17,45,46,51]. The understanding of the origins of so-called large (or high energy) and small (or low-energy) pseudogaps and the effects of these pseudogaps on the normal state properties of doped cuprates represents a serious challenge for a successful theory.

4.1 Formation of a large polaronic pseudogap

The formation of a polaronic superlattice and band with a finite bandwidth restores the translational symmery. At higher doping $x > x_{c2}$ the Bloch-like motion of polarons (or dressed carriers) can occur in this superlattice or polaronic band, whereas the free hole (electron) states of the valence (conduction) band become the excited states. At $x > x_{c2}$ the Fermi level of a new polaronic band lies in the valence (or conduction) band below the ordinary Fermi level of the free electron band. Therefore, the single-particle spectrum of doped HTSC has a pseudogap (i.e., reduction of the DOS near the ordinary Fermi energy) in the normal state. In this case, the large polarons form a degenerate polaronic Fermi-gas (or Fermi-liquid). The strong carrier-phonon interactions lead to the lowering of the electron (or hole) energy (i.e. the chemical potential is shifted) by the value Δ_P or to the polaronic shift of the valence (conduction) band states with opening high-energy polaronic pseudogap Δ_P near the ordinary Fermi surface. So, the ordinary large Fermi surface transforms into the small polaronic one. With decreasing x from $x > x_{c2}$, the polaronic pseudogap transforms into the polaronic insulating gap at $x < x_{c2}$. With increasing x from x_{c2}, the Coulomb repulsion between polarons increases in the metallic state and it leads to the decreasing of the polaronic pseudogap which can be determined from the relation

$$\Delta_P = E_p - e^2/\varepsilon_{eff} R_p, \tag{27}$$

where R_p is the distance between two polarons.

The crossover temperature T_P below which opens the polaronic pseudogap in the excitation

spectrum of doped HTSC can be estimated as

$$k_B T_P \simeq \Delta_P. \tag{28}$$

At $\Delta_P = 0$ we can find the polaronic quantum critical point $x = x_p$ from the relations (27) and (28). This quantum critical point separates two types of Fermi liquids (i.e. Landau and polaronic Fermi liquids). At $E_p \simeq 0.07eV$ and $\varepsilon_{eff} = 25$ we find $R_p \simeq 8.33A$, $x_p = V_a/V_p \simeq 0.24$ (where $V_p = R_p^3 \simeq 570A^3$). For $E_p < 0.07eV$ we obtain $x_p \simeq 0.20$. Many experiments (see [17,37,45,81-83]) have provided evidence for the presence of a finite pseudogap in the overdoped LSCO (with $x \simeq 0.20-0.22$). Transport measurements on overdoped LSCO have show that the characteristic pseudogap temperature T_{PG} is much greater than T_c for $x = 0.22$ [83] and become equal to T_c well into the overdoped regims. The above experimental results indicate that a finite pseudogap observed for $x = 0.20 - 0.22$ vanishes at more higher doping level $x > 0.22$. It is quite likely that such a pseudogap in LSCO is the polaronic pseudogap and disappears at $x = x_p \simeq 0.24$ (cf. experimental results in [84]) in accordance with our prediction. In this HTSC the polaronic pseudogap temperature $T_P \to 0$ at $x \to 0.20 - 0.24$ (see also [51]). Recently, a large pseudogap was observed in different experiments [37,45]. So, the origin of a large pseudogap observed in underdoped, optimally doped and overdoped HTSC can be understood properly within the large D polaron model [48,51]. While the binding energy of a small polaron $E_p(L) = |E_p(L)|$ is expected to be much larger than $0.1eV$ [48]. According to [85] the binding energy of small polarons is about $\simeq 1eV$. In this case the value of x_p should be much larger than 0.24. So, the above pseudogap observed in the excitation spectrum of underdoped, optimally doped and overdoped HTSC cannot be related to the small L polarons.

At $T < T_P$ these HTSC are polaronic metals. They become ordinary metals above the polaronic pseudogap temperature T_P. It is believed that the tetragoral-to-orthorhombic phase transition is also closely related to the ordinary metal-to-polaronic metal (PM) transition at $x = x_p$ (for $T = 0$). Indeed, in LSCO the tetragonal-to-orthorhombic transition occurs at $x \simeq 0.21$ [86] which is close to the above value of $x_p = 0.20 - 0.24$. Resent experimental results [47] are also indicative of the presence of the strong electron-phonon coupling in HTSC and support our results.

4.2 Formation of a small BCS-like non-superconducting pairing pseudogap

At $x < x_p$ the attractive interaction of large D polarons leads to their BCS-like non - SC pairing well above T_c with the formation of k-space large bipolarons. This novel fluctuationless BCS-like pairing scenario above T_c was proposed in [50,53]. The Hamiltonian of the polaronic Fermi-gas with the pair interaction between particles has the form [50]

$$H_F = \sum_{k\sigma} (\epsilon(k) - \mu_F) c^+_{k\sigma} c_{k\sigma} + \frac{1}{2\Omega} \sum_{k,k'} V_F(k - k') c^+_{k\uparrow} c^+_{-k\downarrow} c_{-k'\downarrow} c_{k'\uparrow}, \tag{29}$$

where $\epsilon(k) = \hbar^2 k^2/2m_p$ is the kinetic energy of polarons, μ_F is the chemical potential, $c^+_{k\sigma}(c_{k\sigma})$ is the creation (annihilation) operators of these polarons in the state $|k\sigma>$, k and σ are their wave vector and spin indices, respectively, $V_F(k-k')$ is the pair interaction potential (which has both an attractive and a repulsive part) between large polarons, Ω is the volume of the system.

The Hamiltonian (29) is diagonalized by the standard Bogolubov transformation of Fermi operators. As a result, the elementary excitations in the normal state are well defined quasiparticles with dispersion

$$E_F(k) = \sqrt{\epsilon^2(k) + \Delta_F^2(k)}, \tag{30}$$

where the kinetic energy of polarons $\epsilon(k)$ is measured relative to the chemical potential (including Hartree-Fock energy), $\Delta_F(k)$ is the BCS-like pairing pseudogap determined from

$$\Delta_F(k) = -\frac{1}{\Omega}\sum_{k'} V_F(k-k')\frac{\Delta_F(k')}{E_F(k')} tanh(\frac{E_F(k')}{2k,T)}. \tag{31}$$

In order to find the pairing pseudogap Δ_F and the characteristic pseudogap (or crossover) temperature, we use the BCS-like approximation for $V_F(k,k')$ [50]

$$V_F(k-k') = \begin{cases} V_{FR} - V_{FA} & \text{if } \epsilon(k),\ \epsilon(k') < E_{FA} = E_{bB} + \hbar\omega \\ V_{FR} & \text{if } E_{FA} < \epsilon(k'),\ \epsilon(k') < E_{FR} \\ 0 & \text{if } \epsilon(k) \text{ or } \epsilon(k') > E_{FR}, \end{cases} \tag{32}$$

where E_{FA} and E_{FR} are the cutoff parameters for an attractive V_{FA} (which has both the phonon- and polaron-bag attracting parts) and a repulsive V_{FR} parts of the potential $V_F(k,k')$, respectively, $\hbar\omega$ is the characteristic phonon energy, $E_{FA} << E_{FR}$.

Using the approximation (32), we obtain the following relations for the BCS-like pairing pseudogap Δ_F, crossover temperature T_F and ratio $g_F = 2\Delta_F/k_B T_F$:

$$\begin{aligned} \Delta_F &= (E_{bB} + \hbar\omega)/sinh\left[1/D_F\tilde{V}_F\right], \\ k_B T_F &\simeq 1.14(E_{bB} + \hbar\omega)exp\left[-1/D_F\tilde{V}_F\right] \end{aligned} \tag{33}$$

and

$$g_F = 3.52, \tag{34}$$

where $\tilde{V}_F = V_{FA} - V_{FR}[1 + D_F V_{FR} ln(E_{FR}/E_{FA})]^{-1}$ and D_F are the effective interaction potential and DOS in the polaronic band, respectively.

It should be noted that in many pairing theories the important and crucial link between the (bi)polaronic effect (i.e. bipolaron binding energy E_{bB}) and the BCS-like pairing of carriers is not yet established (see also [67]). In this respect, the above presented pairing theory of polarons is a more general (i.e. generalized) BCS-like theory taking into account not only the combined polaron- and phonon-bag mediated processes but also the novel normal- state pairing of dressed carriers. In the absence of the (bi)polaronic effect that takes place in many low-T_c superconductors, we expect a pure BCS picture with $E_{bB} = 0$. The prefactor in (33) and (34) is nearly doping independent. As the value of E_{bB} decreases with inereasing x and

in the overdoped region $E_{bB} = 0$, whereas the characteristic phonon frequency ω decreases towards $x \to 0$ due to phonon softening [87]. In underdoped and optimally doped HTSC, $T_F >> T_c$ and $T_F > T_c$, respectively, but in overdoped HTSC, $T_F = T_c$ [50,51]. By taking $E_{bB} \simeq 0.04eV$, $\hbar\omega \simeq 0.02eV$ and $D_F\tilde{V}_F \simeq 0.5$ for slightly underdoped and moderate optimally doped LSCO, we find $T_F \geq 100K$. Further, assuming $E_{bB} \sim 0.02eV$, $\hbar\omega \simeq 0.04eV$ and $\tilde{V}_F D_F \simeq 0.25$ for overdoped regime ($n = n_o$), we obtain $T_F \simeq 40K$. With decreasing n, the value of $\tilde{V}_F D_F$ increases as $n^{-2/3}$ [50] and the binding energy $2\Delta_F$ of k-space polaron pairs tends to the binding energy of r-space polaron pairs $E_{bB} + \hbar\omega$ in the strong coupling limit $\tilde{V}_F D_F \geq 0.7$ [49,50]. Therefore, in LSCO the BCS-like pairing pseudogap temperature T_F rapidly increases from $\sim 40K$ (overdoped regime) to $T_F \simeq (E_{bB} + \hbar\omega)/k_B \simeq 700K$ (lightly doped regime with $E_{bB} + \hbar\omega \simeq 0.06eV$). These our results (see Fig.1) are in good agreement with the experimental findings in LSCO [7,39]. So, in underdoped and optimally doped HTSC the BCS-like pairing state of carriers is the novel metallic state but not the SC state. According to the two-stage FBL scenarios of novel superconductivity [50,51] the BCS-like pairing of carriers with flux periods h/2e, diamagnetic effect and without superconductivity can occur at $T_F > T_c$. Indeed, the observed flux periods h/2e and diamagnetic state above T_c in HTSC [88] are well consistent with the above predictions of the FBL model. The value of ε_∞ in YBCO is smaller than in LSCO (see [58]). Therefore, in YBCO the values of E_{bB} and T_F for large D bipolarons are expected to be greater than in LSCO. In Fig. 2, the temperature dependences of the polaronic and BCS-like pseudogaps in underdoped, optimally doped and overdoped HTSC are illustrated.

4.3 Transport properties of large (bi)polarons

The normal state properties of doped HTSC are expected to be sensitive to the formation of the (bi)polaronic pseudogaps. We consider the large D polarons in underdoped and optimally doped HTSC as the degenerate polaronic Fermi-gas in the temperature range $T_F < T < T_P$ and the large bipolarons forming below the BCS-like pseudogap temperature ($T_F > T_c$) as the non-degenerate Bose-gas (BG). Further, we argue that the large D polarons and bipolarons are scattered by the acoustic phonons and impurities (or defects) below T_P and T_F, respectively and have quite different transport properties. The large D polarons existing at relatively high temperature $T > T_F$ are strongly scattered by the same phonons that lead to the polaron formation. It is believed [25] that the mobility of a large polaron is similar in magnitude and temperature dependence to that produced by the scattering of a free electron on acoustic phonons. So, it is reasonable to assume that a large polaron nearly moves as a free particle. Then the scattering probability of large D polarons on acoustic phonons can be calculated by using the well-known relation

$$P(k,k') = \frac{2\pi}{\hbar}| < f|H_{e-ph}|i > |^2\delta(E_f - E_i), \tag{35}$$

where $H_{e-ph} = \sum_{k,q} V_q(a_q - a_q^+)c_{k+q}^+ c_k/N^{1/2}$ is the operator of the electron-phonon interaction, $V_q = iqE_d(\hbar/2M\omega_q)^{1/2}$, ω_q is the phonon frequency with wave vector q, M is the mass of the unit cell, N is the number of the unit cells, $a_q^+(a_q)$ is the creation (annihilation) operator of the phonon, $\delta(E_f - E_i) = \delta(\epsilon_k - \epsilon_{k+q} \pm \hbar\omega_q)$ is the delta function which determines the energy conservation laws. If the wave function of the interacting system in the initial state has the form

$$|i> = \psi_k \Pi_q \phi_{nq}, \tag{36}$$

then after some algebra we obtain

$$P(k,k') = \frac{2\pi V_q^2}{\hbar N}\left[n_q\delta(\epsilon_{k+q} - \epsilon_k - \hbar\omega_q) + (n_q+1)\delta(\epsilon_{k+q} - \epsilon_k + \hbar\omega_q)\right]\delta_{k',k+q}, \tag{37}$$

where n_q is the number of phonons, $\delta_{k',k+q}$ is the delta symbol determines momentum conservation law $k' = k + q$. The energy of polarons is much larger than the energy of acoustic phonons. Therefore, polarons are almost elastically scattered by acoustic phonons and the term $\hbar\omega_q$ in the argument of the delta function can be ignored. Indeed, for small q using the relation $\hbar\omega_q = \hbar v_s q = v_s\sqrt{m_p k_B T}$, we can estimate the ratio $\hbar\omega_q/k_BT$, where v_s is the sound velocity. For $m_p \simeq 2m_e$, $v_s \simeq 10^5 cm/c$ and $T \simeq 200K$, we find $\hbar\omega_q/k_BT \simeq 2.57\cdot 10^{-2} << 1$. Further, the energy of the absorption and emission phonons is negligible in comparison with the Fermi energy of polarons $\epsilon_k = \epsilon_F >> k_BT$. As is obvious from the above estimation, $\hbar\omega_q << k_BT$ and we can use the expansion

$$n_q + 1 \simeq n_q = \frac{1}{exp(\hbar\omega_q/k_BT) - 1} \simeq \frac{k_BT}{\hbar v_s q}. \tag{38}$$

Substituting Eq. (38) into the Eq. (37) we obtain

$$P(k,k') = \frac{2\pi}{\hbar N} 2V_q^2 \frac{k_BT}{\hbar v_s q}\delta(\epsilon_{k'} - \epsilon_k). \tag{39}$$

The total scattering probability of large polarons by acoustic phonons determines the polaron relaxation time

$$\frac{1}{\tau_p(k)} = \sum_{k'} P(k,k')[1 - cos(k',k)]. \tag{40}$$

At the elastic scattering of polarons, the vectors k and k' with the angle α between them lie on the same energy surface. Going in (40) from summation to integration and making some elementary transformations we obtain

$$\frac{1}{\tau_p(k)} = \frac{2V_q^2 k_BT v_0 m_p}{\pi\hbar^4 v_s}\int\int\left(-\frac{q}{k}cos\alpha\right)\frac{1}{kq^2}\delta\left(\frac{q}{2k} + cos\alpha\right)sin\alpha d\alpha q^2 dq, \tag{41}$$

where v_0 is the volume of the unit cell.

Here two spin orientations of polarons are taken into account. The calculation of the integral (41) gives

$$\tau_p(\epsilon) = \frac{\pi\rho_M\hbar^4 v_s^2}{E_d^2(2m_p)^{3/2}k_BT\epsilon^{1/2}}, \tag{42}$$

where $\rho_M = M/v_0$.

The average relaxation time of polarons is determined from

$$< \tau_p >= \frac{\int_0^\infty \epsilon^{3/2}(\partial f_0/\partial\epsilon)\tau(\epsilon)d\epsilon}{\int_0^\infty \epsilon^{3/2}(\partial f_0/\partial\epsilon)d\epsilon}, \tag{43}$$

where f_0 is the distribution function of Fermi particles.

At $\epsilon \neq \epsilon_F$ and $\epsilon = \epsilon_F$ we can assume $\partial f_0/\partial\epsilon = 0$ and $\partial f_0/\partial\epsilon \simeq \delta(\epsilon - \epsilon_F)$, respectively. Therefore, $< \tau_p >$ is equal to $\tau_p(\epsilon_F)$.

Then the conductivity and resistivity are determined as

$$\sigma = en\mu_p = \frac{\pi\hbar^4 e^2 n\rho_M v_s^2}{E_d^2 m_p (2m_p)^{3/2} k_B T \epsilon_F^{1/2}} \tag{44}$$

and

$$\rho = \frac{1}{\sigma} = \frac{E_d^2 m_p (2m_p)^{3/2} k_B T \epsilon_F^{1/2}}{\pi\hbar^4 e^2 n\rho_M v_s^2} \tag{45}$$

At relatively high temperature (i.e. $T_F < T < T_P$), the scattering is dominated by acoustic phonons and the mobility of large polarons decreases with temperature as $\mu_p \sim 1/T$. While at low temperatures $T < T_F$ the scattering of large bipolarons by ionized impurities (or defects) is the dominated mechanism. This scattering process of large bipolarons can be described by the Conwell-Weisskopf model of Rutherford scattering from the Coulomb potential

$$V(r) = \frac{Z_1 Z_2 e^2}{\varepsilon_{eff} r}, \tag{46}$$

where Z_1 and Z_2 are the charges of the impurity and bipolaron, respectively. The calculation of the scattering cross-section in the Conwell-Weisskopf approximation [89] gives the following relation for the relaxation time of bipolarons

$$\tau_I(\epsilon) = \frac{\sqrt{2}\varepsilon_{eff}^2 m_B^{1/2} \epsilon^{3/2}}{\pi n_I (Z_1 Z_2 e^2)^2 ln\left[1 + (\varepsilon_{eff}\epsilon/n_I^{1/3} Z_1 Z_2 e^2)^2\right]}, \tag{47}$$

where n_I is the concentration of the impurities, m_B is the mass of bipolarons. The average relaxation time of bipolarons is calculated from the expression

$$< \tau_I >= \int_0^\infty \epsilon^{3/2} exp(-\epsilon/k_B T)\tau_I(\epsilon)d\epsilon / \int_0^\infty \epsilon^{3/2} exp(-\epsilon/k_B T)d\epsilon \tag{48}$$

The logarithmic term in (47) is nearly constant and in this term ϵ can be relaced by that value for which the integrand $\epsilon^3 exp(-\epsilon/k_B T)$ is a maximum. This is true for $\epsilon = 3k_B T$. Then from the Eq. (48) we obtain the following relation

$$< \tau_I >= \frac{8\sqrt{2}(k_B T)^{3/2} \varepsilon_{eff}^2 m_B^{1/2}}{\pi^{3/2} Z_1 Z_2 e^2 n_I ln\left[1 + (3\varepsilon_{eff} k_B T/n_I^{1/3} Z_1 Z_2 e^2)^2\right]}. \tag{49}$$

At $3k_BT\varepsilon_{eff}T < n_I^{1/3}Z_1Z_2e^2$ the temperature dependence of the logarithmic term becomes essential. At $\varepsilon_{eff} \simeq 25$, $n_I \simeq 0.5 \cdot 10^{21}cm^{-3}$, $Z_1 = 1$ and $Z_2 = 2$ we can expand the logarithmic term for $T < 350K$. In the case $T_F < 300K$, the mobility of large bipolarons is given by

$$\mu_b \simeq \frac{16\sqrt{2}e}{9\pi^{3/2}n_I^{1/3}(k_BT)^{1/2}m_B}. \tag{50}$$

The temperature dependence of the resistivity of underdoped and optimally doped HTSC in the temperature range $T_c < T < T_F$ is expected to be $\rho \sim \sqrt{T}$. At higher temperature $T > T_P$, the undressed (i.e. free) carrier exist in these HTSC as well as in overdoped HTSC and the carrier-carrier interaction seems to be the dominated scattering mechanism. In this case we can expect the dependence $\rho \sim T^2$ above T_P at least in optimally doped and overdoped HTSC. Indeed, the temperature dependence $\rho \sim T^2$ was observed at $T > 650K$ in HTSC [73,91]. The resulting temperature dependence of ρ in optimally doped HTSC is shown in Fig. 3. The above temperature dependences of $\rho \sim T$ (at $T_F < T < T_P$) and $\rho \sim T^{1/2}$ (at $T_c < T < T_F$) are in good agreement with various experimental findings [17,72]. We believe that in the underdoped regime close to the doping level x_{c2} (i.e. MIT boundary) the increasing of the insulating (static) stripes (see below) leads to the semiconductor-like behaviour of the resistivity. Such a temperature dependence of ρ was also observed in HTSC [90].

4.4 Magnetic susceptibility

The pseudogap formation in the excitation spectrum of doped HTSC manifests itself also in the Pauli spin susceptibility which is determined from the relation

$$\chi_p = -\int_0^\infty 2\mu_B^2 \frac{\partial f_h}{\partial \epsilon} D(\epsilon)d\epsilon, \tag{51}$$

where $f_h(\epsilon) = \{exp[(\Delta_P + \epsilon)/k_BT] + 1\}^{-1}$ is the distribution function of hole polarons, ϵ is their kinetic energy measured relative to the Fermi energy ϵ_F, $D(\epsilon)$ is the DOS at the Fermi level, μ_B is the Bohr magneton.

After some transformation the Eq. (51) can be written in the form

$$\chi_p = 2\frac{\mu_B^2}{k_BT}\int_0^\infty \frac{exp\left[-(\Delta_P + \epsilon)/k_BT\right]}{\left\{1 + exp\left[-(\Delta_P + \epsilon)/k_BT\right]\right\}^2}\epsilon^{1/2}d\epsilon. \tag{52}$$

At $exp\left[-(\Delta_P + \epsilon)/k_BT\right] < 1$ using the expansion $\left\{1 + exp\left[-(\Delta_P + \epsilon)/k_BT\right]\right\}^{-2} \simeq 1 - 2exp\left[-(\Delta_P + \epsilon)/k_BT\right]$, we have

$$\chi_p \simeq \frac{2\mu_B^2}{k_BT}\int_0^\infty \{1 - 2exp\left[-(\Delta_P + \epsilon)/k_BT\right]\}exp\left[-(\Delta_P + \epsilon)/k_BT\right]\epsilon^{1/2}d\epsilon =$$

$$= \sqrt{\pi k_BT}exp(-\Delta_P/k_BT)\left[1 - exp(-\Delta_P/k_BT)/\sqrt{2}\right] \tag{53}$$

We see that the magnetic susceptibility is decreased exponentially below the polaronic pseudogap temperature T_P. Now we determine χ_p below the BCS-like pairing pseudogap temperature T_F from the relation

$$\chi_p = -2\mu_B^2 \int_0^\infty D(\epsilon) \frac{\partial f}{\partial \epsilon} d\epsilon, \tag{54}$$

where $f(\epsilon) = \left[exp(\sqrt{\epsilon^2 + \Delta_F^2}/k_BT) + 1\right]^{-1}$ is the Fermi function.

We can transform the Eq. (54) to

$$\chi_p = 2\frac{\mu_B^2}{k_BT} \int_0^\infty \frac{exp(-\sqrt{\epsilon^2 + \Delta_F^2}/k_BT)}{\left[1 + exp(-\sqrt{\epsilon^2 + \Delta_F^2}/k_BT)\right]^2} \cdot \frac{\epsilon}{\sqrt{\epsilon^2 + \Delta_F^2}} D(\epsilon) d\epsilon \tag{55}$$

As is generally known the main contribution to the BCS-like pairing comes from the energy region close to the Fermi level and $D(\epsilon)$ can be replaced by the constant $D_F = D(\epsilon_F)$. Therefore, the *Eq.* (55) after expansion of the expression $\left[1 + exp(-\sqrt{\epsilon^2 + \Delta_F^2}/k_BT)\right]^2$ in a power series of $y = exp(-\sqrt{\epsilon^2 + \Delta_F^2}/k_BT)$ may be written as

$$\chi_p \simeq 2\mu_B^2 \int_{\Delta_F^*}^\infty exp(-y)\left[1 - 2exp(-y)\right] dy =$$

$$= 2\mu_B^2 exp(-\Delta_F/k_BT)\left[1 - exp(-\Delta_F/k_BT)\right]. \tag{56}$$

It is abvious that in underdoped and optimally doped HTSC the magnetic susceptibility below the lower crossover temperature T_F decreases also exponentially and faster than above T_F (see Fig.4). The above results are in good agreement with the experimental observations (see [12,46,84]).

5 Novel pseudogapped superconducting states

The mechanism of high-T_c superconductivity in doped cuprates has been discussed in terms of the BCS-like s-, p- and d-wave pairing of carriers [17,21-24], BEC of an ideal BG of r-space pairs or bipolarons [17,24-26], BEC-BCS crossover [27], spin-charge separation [10,28,29,74,75], SF condensations of attracting k-space composite bosons (i.e. cooperons and bipolarons) [50,51] and AF spin fluctuations [46]. In many theoretical models the main attention had been focused to different intermediate (i.e. pre-superconducting or precursor) states. There different k- and r-space pairing mechanisms are discussed. While the true SF condensations (i.e. PC and SPC) of attracting composite bosons leading to their superconductivity are not at all considered. The PC of attracting holons has been discussed only in some versions of the RVB models [92,93]. The SPC and PC of attracting cooperons and bipolarons were studied only within the novel two-stage FBL model [50,51]. In particular, it has been proposed that in conventional superconductors without (bi)polaronic effects the Cooper-pair formation and the true SF condensation of attracting cooperons occur simultaneously at the same temperature $T_F = T_B = T_c$ [50,53]

(where T_B is the SF condensation temperature of attracting composite bosons). Therefore, it is difficult to distinguish the transient (pre-superconducting) BCS and the true SF states of Cooper pairs. The BCS pairing gap in the excitation spectrum of the conventional superconductors appears also at T_c. For this reason the BCS theory was quite successful in describing SC properties of these materials, although it ignores the distinction between the Cooper-pair formation discribed by BCS order parameter Δ_F and the true SF condensation of cooperons described by SF condensate order parameter Δ_B [50]. Nevertheless, the distinction between the Cooper-pair formation and the SF condensation of cooperons was observed even in conventional superconductors as the non-zero DOS in the BCS gap [94] and the above-gap structure [95]. The evident inconsistency of the BCS-like pairing models in the description of SC (or SF) states (i.e. first- and second-order SC or SF phase transitions) was observed both in doped HTSC [17,36-40] and in ^3He [96]. The formation of a pseudogap well above T_c in underdoped and optimally doped HTSC is also indicative of this. Many theories of the pseudogap based on the SC fluctuations (see [27,73,78-80]) suggest that the SC gap below T_c evolves smoothly into the pseudogap above T_c without closing at T_c. However, the second-order SC transition and abrupt changes (i.e. jumps) of specific heat and other termodynamic parameters at T_c observed in underdoped and optimally doped HTSC cannot be reconciled with these theories. Moreover, recent experiments on HTSC show [15,97-99] that the SC gap and the normal state pseudogap have different origins and coexist below T_c. The coexistence of the pseudogap and the SC gap below T_c was predicted very early [50,51,53]. The RVB model may also explain these experimental findings. But, other experimental facts show [12,39,69] that the pseudogap observed in HTSC is not a spin-gap only. Further, it is difficult to describe the normal and state properties of single-layered cuprates and the origin of the large pseudogap in terms of this model. While the novel BCS-like pairing of carriers and the opening of the low-energy pairing pseudogap Δ_F semultaneously both in the charge and spin channel well above T_c predicted first in [50,51,53] is observed now experimentally as the Bose-type species with charge 2e and diamagnetic effect above T_c [88]. So, the superconductivity due to the so-called SPC and PC of attracting composite bosons described by novel two-stage FBL model seems to be a very promising approach to the problem. The relationship between the pairing pseudogap and the true SC gap in underdoped, optimally doped and overdoped HTSC is not clear enough at the moment and further studies within the novel two-stage FBL model are cleary necessary.

5.1 Hamiltonian of Fermi-Bose-liquid

In superconductors (including also ^3He) the unpaired and paired Fermi particles can exist (or coexist) as the FBL. The total Hamiltonian of a mixed FBL system has the form

$$H = H_F + H_B + H_{FB}, \tag{57}$$

where H_F and H_B are the Hamiltonians of Fermi and Bose subsystems, respectively, H_{FB} is the interaction between these subsystems.

In a mixed FBL only the total number of particles is conserved and the chemical potential is determined from $N = N_F + 2N_B$, where N_F and N_B are the number of Fermi and Bose particles, respectively. The diagonalization of the Hamiltonian (57) and its subsequent investigation are very complicated problem. Therefore, there are two different approaches to this problem. First of these approaches has been proposed in [100,101], where only fermion-boson interaction H_{FB} is taken into account without interfermion and interboson interactions in H_F and H_B. It allows to obtain the modified BCS-like excitation spectrum of Fermi-liquid which is combined with the BEC of an ideal BG of r-space pairs. While the second approach has been proposed in [50,51] where the fermion-fermion and boson-boson interactions are taken into account without fermion-boson interaction. In this FBL model the upper broad band of fermions (or polarons) may coexists with the lower relatively narrow band of Bose (or bipolaron) particles. When the bipolaronic band energy is decreased below the polaronic Fermi level, polarons will flow into it forming composite bosons. The polaron-bipolaron phase-separation takes place just as the phase separation in the mixed $^3He - ^4He$ system or spin-charge system (in RVB models). This leads to the novel two-stage FBL scenario of superconductivity. So, the separate consideration of the Fermi and Bose subsystems with fixed N_F and N_B is justified. The phase separation can take place even in conventional superconductors, where there are two different velocities of unpaired fermions and Cooper pairs. In Fermi systems, superconductivity would emerge in two stages: first the BCS-like pairing of carriers (e.g. free electrons or holes and polarons) leads to the formation of the transient or normal state k-space pairs below T_F and then follows the SF phase transition at SPC of attracting cooperons below $T_B = T_c$ (e.g. in conventional superconductors and overdoped HTSC) or follow two successive SF phase transitions (e.g. in underdoped and optimally doped HTSC) of these composite bosons (i.e. bipolarons) at their attractive PC below T_B and SPC below the characteristic crossover temperature $T = T_B^* < T_B$. In this two-stage FBL model, a SF Bose-liquid's condensate and excitations are unlike those of an ideal BG of cooperons and bipolarons discussed in the BCS-like (s-, p- and d-wave) pairing and BEC theories in which key intercooperon and interbipolaron interactions are fully ignored. We consider the SF condensation phenomena of composite bosons within the proper boson mean field theory. We note that the conventional BEC of an ideal BG of any composite or non-composite bosons is irrelevant to superconductivity (superfluidity)(see [48,50,51,53]).

5.2 Superfluid condensations of attracting composite bosons

The pair Hamiltonian of an attractive Bose system can be written as [50]

$$H_B = \sum_k \left[\epsilon(k) a_k^+ a_k + \frac{1}{2} \Delta_B(k) (a_k^+ a_k^+ + a_k a_{-k}) \right], \tag{58}$$

where $\tilde{\epsilon}(k) = \epsilon(k) - \mu_B + V_B(0)\rho_B + \chi_B(k)$, $\epsilon(k) = \hbar^2 k^2/2m_B$, $\Delta_B(k) = (1/\Omega)\sum_{k'} V_B(k-k') < a_{-k'}a_{k'} >$, $\chi_B(k) = (1/\Omega)\sum_{k'} V_B(k-k')f_B(k')$, $f_B(k) =< a_k^+ a_k >$, $n_B = (1/\Omega)\sum_k f_B(k)$, μ_B^o is the chemical potential of an BG, a_k^+ and a_k are the boson creation and annihilation operators, respectively, $V_B(k-k')$ is the interboson interaction potential. The Hamiltonian (58) can be diagonalized by the Bogolubov transformations of Bose operators. After some elementary transformations, we obtain the excitation spectrum of attracting bosons in the form

$$E_B(k) = \sqrt{\tilde{\epsilon}^2(k) - \Delta_B^2(k)}, \tag{59}$$

where $\Delta_B(k)$, μ_B^o and $\chi_B(k)$ are determined from the coupled integral equations

$$\begin{aligned}
\Delta_B(k) &= -\frac{1}{\Omega}\sum_{k'} V_B(k-k')\frac{\Delta_B(k')}{2E_B(k')} coth\frac{E_B(k')}{2k_BT} \\
N_B &= \sum_k n_B(k) = \sum_k \left[\frac{\tilde{\epsilon}(k)}{2E_BT} coth\frac{E_B(k)}{2k_BT} - \frac{1}{2}\right] \\
\chi_B(k) &= \frac{1}{\Omega}\sum_{k'} V_B(k-k')\left[\frac{\tilde{\epsilon}(k')}{2k_BT} - \frac{1}{2}\right]
\end{aligned} \tag{60}$$

by means of their self-consistent solution.

At $E_B(0) = 0$ or $-\mu_B^o + V_B(0)\rho_B + \chi_B(0) = |\tilde{\mu}_B| = \Delta_B(0)$ the terms of the sums (60) with $k = 0$ and $k' = 0$ should be considered separately according to the procedure proposed in [102]. Further, in order to solve the equations (60) we can approximate the interboson interaction potential $V_B(k-k')$ in the simple separable form as is done in BCS-like pairing theory [50]

$$V_B(k-k') = \begin{cases} V_{BR} - V_{BA} & \text{if } 0 \le \epsilon(k),\ \epsilon(k') < \xi_{BA} \\ V_{BR} & \text{if } \xi_{BA} \le \epsilon(k) \text{ or } \epsilon(k') < \xi_{BR} \\ 0 & \text{if } \epsilon(k),\ \epsilon(k') > \xi_{BR}, \end{cases} \tag{61}$$

where ξ_{BA} and ξ_{BR} are the cutoff parameters for attractive and repulsive parts of the potential $V_B(k-k')$, respectively.

This approximation allows us to carry out the calculations thoroughly and these detail calculations give us a new insight to the problem of SF condensations or on the basic properties of a SF Bose-liquid. The quantitative calculations are carried out for $\xi_{BR} >> \xi_{BA} >> |\tilde{\mu}_B| \sim \Delta_B \sim k_BT_B$. Here T_B is the mean-field temperature characterizing the appearance or disappearance of a SF condensate order parameter Δ_B. While ξ_{BA} characterizes the thickness of a SF condensation layer including almost all Bose particles. As the main contribution to the $\Delta_B(k)$, N_B and $\chi_B(k)$ comes from the small values of $k < k_A$, whereas the large values of $k > k_A$ give small corrections that may be neglected. When two Bose particles in a diluted BG interact with each other, the binding energy E_b of these particles is determined from the equation

$$\tilde{V}_B \sum_k \frac{1}{2\epsilon(k) - E_b} = 1, \tag{62}$$

where

$$\tilde{V}_B = V_{BA} - V_{BR}[1 + V_{BR}I_R]^{-1} \tag{63}$$

From (62) at $\xi_{BA} >> E_b$ we find $I_R = \frac{1}{2} D_B ln(\xi_{BR}/\xi_{BA})$, $D_B = m_B/2\pi\hbar^2$ and $I_R \simeq D_B\,[\sqrt{\xi_{BR}} - \sqrt{\xi_{BA}}]$, $D_B = \sqrt{2} m_B^{3/2}/2\pi^2\hbar^3$ for 2d- and 3d-BG, respectively [50]. Further, the following coupling constants $\gamma_B = \tilde{V}_B D_B \sqrt{\xi_{BA}}$ and $\gamma_B = \tilde{V}_B D_B$ can be introduced for 3d- and 2d-BG, respectively.

5.2.1 Superfluid pair condensation of attracting three- and two-dimensional bosons

We first discuss the PC of attracting 3d and 2d bosons. In (60) going from summation to integration on ϵ and calculating the integrals we can determine the following critical values of interboson coupling constants for the appearance of the energy gap $\Delta_{SF} = \sqrt{\tilde{\mu}_B^2 - \Delta_B^2}$ in the excitation spectrum of attracting 3d bosons [50]

$$\gamma_B^* = 2.404 \sqrt{\frac{k_B T_{BEC}}{\xi_{BA}}} + \sqrt{1 + \frac{5.779 k_B T_{BEC}}{\xi_{BA}}} \tag{64}$$

and 2d bosons [92]

$$\gamma_B^* = \frac{1}{sinh^{-1}\sqrt{\xi_{BA}/4k_B T_0}}, \tag{65}$$

where $T_{BEC} = 3.31\hbar^2 n_B^{2/3}/k_B m_B$ is the BEC temperature of an ideal 3d-BG, $T_0 = 2\pi\hbar^2 n_B/k_B m_B$ is the BEC-like temperature of an ideal 2d-BG. The numerical solutions of the coupled integral equations (60) for $\gamma_B > \gamma_B^*$ exhibit only PC of attracting 3d- and 2d-bosons as the second-order SF phase transitions at $T = T_B$ without any features of the order parameter Δ_B below T_B. The SF condensation temperatures of attracting 3d- and 2d-bosons are determined from the relations [50]

$$x^{3/2} - 2.13\gamma_B x^2 \sqrt{k_B T_{BEC}/\xi_{BA}} = 1 \tag{66}$$

and

$$T_B = -\frac{T_0}{ln[1 - exp(-2\gamma_B/(2+\gamma_B))]}, \tag{67}$$

respectively, where $x = T_B/T_{BEC}$.

The temperature dependences of $\tilde{\mu}_B$ and Δ_B for attractive 3d- and 2d-BG were studied in [50] for two limit cases $T \ll T_B$ and $T \to T_B$. In particular, in an attractive 3d-BG the temperature dependences of $\tilde{\mu}_B$ and Δ_B near T_B have the forms

$$\tilde{\mu}_B(T) \simeq |\tilde{\mu}_B(T_B)| \left[1 + a_B \left(\frac{T_B - T}{T_B}\right)^{0.5}\right], \tag{68}$$

and

$$\Delta_B(T) \simeq 2|\tilde{\mu}_B(T_B)|\sqrt{a_B} \left(\frac{T_B - T}{T_B}\right)^{0.25}, \tag{69}$$

where $a_B = 2(\pi^{3/2}\gamma_B/3.912)^{-0.5}(\xi_{BA}/k_B T_{BEC})^{0.25}$.

The temperature dependences of $\tilde{\mu}_B$ and Δ_B for attractive 3d- and 2d-BG are presented in Fig.5.

5.2.2 Superfluid single particle condensation of attracting 3d and 2d composite bosons

At $\gamma_B < \gamma_B^*$ the numerical solutions of the Eqs. (60) by means of the BCS -like approximation (61) (see [50]) exhibit the second-order SF phase transition at $T = T_B$ and then the first-order SF phase transition at SPC temperature $T = T_B^* < T_B$, where the energy gap Δ_{SF} in $E_B(k)$ vanishes both for a 3d-BG and for a 2d-BG. The characteristic SPC temperature T_B^* of attracting 2d bosons is equal to zero (at $\gamma_B < \gamma_B^*$). While, in an attractive 3d-Bose system $T_B^* \neq 0$ and there Δ_B has the pronounced (at $\gamma_B << \gamma_B^*$) and some cases (when $\gamma_B < \gamma_B^*$) not very pronounced kink-like temperature dependence (Fig.6) near T_B^*. In the limit cases $\gamma_B < \gamma_B^*$ (strong interboson coupling) and $\gamma_B \ll \gamma_B^*$ (weak interboson coupling) the characteristic crossover temperatures T_B^* in a 3d-SF Bose-liquid are close to $T = 0$ and $T = T_B$, respectively. The temperature dependences of $\tilde{\mu}_B$ and Δ_B near the first-order SF phase transition temperature $T_B^* < T_B$ ($\gamma_B \ll \gamma_B^*$) has the form [50]

$$|\tilde{\mu}_B(T)| = \Delta_B(T) = |\tilde{\mu}_B(T_B^*)| \left[1 + b\left(\frac{T_B^* - T}{T_B^*}\right)^{0.5}\right], \tag{70}$$

where $b = (\pi^{3/2}\gamma_B/3.912)^{-0.5}(\xi_{BA}/k_B T_B^*)^{0.25}$.

In a 3d-SF Bose-liquid the values of γ_B^* are approximately equal to 2.0, 1.7 and 1.4 for $\xi_{BA}/k_B T_{BEC} = 10, 20$ and 50, respectively. We emphasize that at $\gamma_B < \gamma_B^*$ the first-order SF phase transitions SPC$\leftrightarrow$PC of attracting 3d-bosons occur at $T = T_B^* \ll T_B$ with $T_B^* < T_{BEC}$. While, at $\gamma_B \ll \gamma_B^*$ such phase transitions take place near T_B with $T_{BEC} < T_B^* < T_B$.

At $\gamma_B \ll \gamma_B^*$ the energy gap Δ_{SF} in the excitation spectrum of attracting 3d bosons appears some below T_B (i.e. above T_B^*) and its quantity is determined from the relation [50]

$$\Delta_{SF}(T) = |\tilde{\mu}_B(T_B)| \left[1 - a_B\left(1 - \frac{T}{T_B}\right)^{0.5}\right]. \tag{71}$$

For $\gamma_B < \gamma_B^*$ the energy gap Δ_{SF} always exists in the excitation spectrum of attracting 2d bosons at $T > 0$ [92] and its quantity is expected to be larger than such a gap in the excitation spectrum of attracting 3d bosons. The presence or absence of this energy gap in the excitation spectrum of attracting 3d and 2d bosons determines the structure of the SF states both in superconductors and in quantum liquids.

5.3 Relationship between the pairing pseudogap and the true superfluid condensate gap in high-T_c superconductors

To determine the origin and the nature of the normal and SC states both in conventional superconductors and in HTSC first of all we should understand properly the physical essence of the pairing order parameter Δ_F, the SF condensate order parameter Δ_B and the energy gap Δ_{SF} in the excitation spectrum of a SF Bose-liquid in different cases. As the relationship between the low-energy pseudogap Δ_F and the SC gaps Δ_B and Δ_{SF} undoubtedly plays an

important role in establishing possible scenarios of superconductivity in doped HTSC as well as in determining the nature of the novel normal and SC states in these materials.

5.3.1 Two possible Fermi-Bose-liquid scenarios of novel superconductivity and their experimental evidences

In Fermi systems (all superconductors and ^3He are the same), the novel superconductivity (superfluidity) results from the coexistence of two distinct order parameters Δ_F and Δ_B which characterize the attracting fermion pairs and composite boson pairs, respectively. The coexistence of the order parameter Δ_F and Δ_B predicted first in [50,53] and observed now experimentally in [15,97-99] is the main criterion for the appearance of superconductivity (superfluidity) in any Fermi systems. In Fermi systems two types of novel superconductivity can be realized by two FBL scenarios [50,51]. One of these FBL scenarios is realized in so-called fermion superconductors (FSC), where the formation of k-space pairs and the SF condensation of these composite bosons occur at the same temperature $T_c = T_F = T_B$. Another FBL scenario of novel superconductivity is realized in so-called boson superconductors (BSC), where the formation of k-space pairs and the SF condensation of these composite bosons take place at different temperatures $T = T_F > T_B = T_c$ and $T = T_B = T_c$. The doped cuprates and other superconductors (including low-T_c, organic and heavy fermion superconductors) can be classified either as the FSC or as the BSC [50,51]. When in superconductors the SF condensation or SC transition temperature T_c is determined by the depairing temperature T_F of bound fermions, these systems are called as the FSC. However, if in superconductors the SC transition temperature is determined by the SF condensation temperature T_B of composite bosons, these systems are called as the BSC.

In BSC (i.e. underdoped and optimally doped HTSC) the strong carrier-phonon interactions (or (bi)polaronic effects) are responsible for the separation of the pair formation temperature T_F and SF condensation temperature $T_B = T_c$. There two crossover temperatures T_P and T_F exist above T_c, whereas another crossover temperature T_B^* would exist below T_c. In BSC the BCS-like pairing pseudogap Δ_F opens in $E_F(k)$ well above T_c and persists in the SC state, while the true SC (i.e. SF condensate) gap Δ_B appears only below T_c within the low-energy pseudogap Δ_F (Fig.7) [50]. So, the pairing pseudogap Δ_F is different from the SC gap Δ_B in its origin. This pseudogap opening above T_c smoothly evolves into the SC state pseudogap and it is not a precursor to the SC gap. In contrast, the existing theories of the pseudogap in cuprates based on the SC phase fluctuations and BCS-BEC crossover scenarios erroneously suggest that the normal-state pseudogap has the same origin as the SC gap. They in doing so currently assert that the SC gap below T_c evolves smoothly into the pseudogap above T_c. However, recent experiments [15,18,97-99,103] confirm our above presented results and earlier predictions [50,51,53], and disagree with the conclusions of the SC phase fluctuation and BCS-BEC crossover models as well as with the composite gap $\sqrt{\Delta_{SC}^2 + \Delta_{PG}^2}$ models (where any pseudogap Δ_{PG} is assumed).

With weakening of the (bi)polaronic effects, T_F approaches T_B and merges with the T_c in FSC (i.e. overdoped HTSC) in which the low-energy BCS-like pairing pseudogap exists only below T_c but the high-energy non-pairing polaronic pseudogap can exist above T_c. Indeed, many experimental results [8,9,15,17,18,37,38] confirm also this physical picture in overdoped HTSC. The quantity of the pairing pseudogap Δ_F may be larger or smaller than the SC gap Δ_B (Fig.7) depending on the doping level or strength of the carrier-phonon interactions. At $\Delta_F > \Delta_B$ the SC gap is manifested as the non-zero DOS in the BCS-like pairing pseudogap Δ_F. Further, the excitations of a 3d-SF Bose-liquid at $\Delta_{SF} = 0$ (or $T < T_B^*$) and $\Delta_{SF} \neq 0$ (or $T > T_B^*$) are manifested as the non-zero DOS in the bottom (i.e. zero-bias conductance peak (ZBCP)) and inside of the BCS-like energy gap Δ_F (e.g. splitting of ZBCP). These key features of SF condensate gap Δ_B and low-energy gap Δ_{SF} were also clearly observed in HTSC [37,43,44]. According to the above presented SF Bose-liquid model the energy gap Δ_{SF} increases under the magnetic field and appears above $T_B^* \simeq 0.7T_c$ (at $\gamma_B << \gamma^*$) (see [50]). Recent by of the suppression of ZBCP by the applied magnetic fields [104] and its disappearance at $T \simeq 0.7T_c$ [105] were observed in accordance with our predictions. Such anomalous SC state properties cannot be understood properly within the BCS-like s-, p- and d-wave pairing models. In particular, the gapless superconductivity in all superconductors and superfluidity in ^3He are caused by the gapless excitation spectrum of 3d composite bosons at $T \leq T_B^*$ and not by the presence of point or line nodes of the BCS-like gap Δ_F assumed in some p- and d-wave pairing models. The PC→SPC phase transition at $T = T_B^* < T_c$ both in HTSC and in ^{3}He is accompanied by the vanishing of the gap Δ_{SF}. It is another SF (or SC) phase transition. So, in HTSC two types of SC (or SF) states can be formed as the A- and B-phases just as in ^{3}He [96] and heavy-fermion superconductors [106].

The first-order SPC→PC phase transition in an attractive 3d-BG of composite bosons can take place in BSC at $\gamma_B << \gamma_B^*$. It is accompanied by radical changes of many SC parameters and should be manifested as the λ-like jumps in specific heat and the kink-like temperature dependences of the critical magnetic fields H_{c1}, H_c and H_{c2} (see [50]). Indeed, the first-order SC phase transition and the anomalies of SC parameters were observed at $T = (0.4 - 0.8)T_c$ in HTSC [40-42,107,108]. The first-order SC phase transition or SPC→PC phase transition in an attractive 3d-BG leads to the opening of the energy gap Δ_{SF} in the excitation spectrum of attracting 3d composite bosons at $T > T_B^*$ with the half-integer h/4e magnetic flux quantization. We emphasize that the energy gap Δ_{SF} opening in the excitation spectrum of a 2d-SF Bose-liquid at $T > 0$ is always larger than such a gap opening in the excitation spectrum of a 3d-SF Bose-liquid at $T > T_B^*$ [50,51]. For this reason, the half-integer h/4e magnetic flux quatum should be manifested much better in the 3d-2d crossover region (e.g. grain boundaries in HTSC) than in the 3d region. Indeed, such h/4e magnetic flux quantum was observed in the grain boundaries and in thin films of some HTSC [13]. Further, in BSC the second-order SC phase transition at $T_B = T_c$ predicted our SF Bose-liquid model is the λ-like phase transition,

but not the step-like BCS-like one. This distinctive feature of the SC phase transition is also observed in HTSC, organic and heavy-fermion superconductors (see [50]). In the weak coupling FSC, the SC energy gap Δ_B may be larger than the pairing pseudogap Δ_F (see below) and it can be manifested as the above-gap structure. Such an above-gap structure was observed in conventional superconductors [95]. We believe that Δ_B can be also observed in heavily overdoped HTSC as the above-gap structure. Apparently, in some FSC (e.g. heavily overdoped HTSC and conventional superconductors) with $\gamma_B << 1$, the energy gap Δ_{SF} in $E_B(k)$ appears near $T_B = T_c$, where $\Delta_{SF} > \Delta_F$ and both the second-order pre-superconducting BCS-type transition and the true SC phase transition take place simultaneously with the step-like jump of the specific heat.

5.3.2 Relationship between the pairing pseudogap and the true SC gap and their doping dependences

We now examine the relationship between the BCS-like pairing pseudogap Δ_F and the SF condensate gap Δ_B as a function of the doping concentration and find the basic and distinctive regularities of the pseudogap formation and the true SC transition phenomena in underdoped, optimally doped and overdoped HTSC. In order to find the doping dependence of the BCS- like pairing pseudogap

$$\Delta_F(n) = \frac{E_{bB} + \hbar\omega_D}{sinh\left[1/D_F(n)\tilde{V}_F\right]}, \tag{72}$$

we can approximate the DOS in a simple form [50]

$$D_F(\epsilon) = \begin{cases} 1/\epsilon_F & \text{if } \epsilon < \epsilon_F \\ 0, & \text{otherwise.} \end{cases} \tag{73}$$

Further, for simplicity, we restrict ourselves to the case when $\tilde{V}_F$ is doping independent. Then we can find the approximate doping dependences of the pseudogap Δ_F in the form

$$\Delta_F(n) = \frac{E_{Bb} + \hbar\omega_D}{sinh\left[\hbar^2(3\pi^2 n)^{2/3}/2m_p\tilde{V}_F\right]}. \tag{74}$$

As can be seen Δ_F decreases rapidly with increasing carrier (polaron) concentration n. At $n > n_{c2}$ we consider the doping dependences of the SC order parameter Δ_B within the above boson mean-field theory. As n is increased from n_{c2}, the thickness ξ_{BA} of the condensation layer ($\xi_{BA} = 0$ for $n < n_{c2}$) including almost all Bose particles gradually increases, while $\tilde{V}_B$ would decrease. So, we can assume that $\tilde{V}_B\sqrt{\xi_{BA}}$ is almost doping in dependent up to n_o. Then in an attractive 3d-BG the effective interboson coupling strenght γ_B depends on the DOS of composite bosons D_B and increases with increasing n_B. As the effective mass of interacting bosons $m_B^* = m_B\left[1 - n_B V_B(0)/\xi_{BR}\right]^{-1}$ [50] increases with increasing n_B. The relation $\Delta_B \simeq n_B V_{BA}$ holds for the weak interboson coupling $\gamma_B << \gamma_B^*$ [109]. Numerical calculations show [50] that the ratio $2\Delta_B/k_B T_B \sim \gamma_B$. So, as the doping concentration n (or n_B) is increased from n_{c2}, the increasing of the interboson coupling strenght γ_B and the SF

condensate order parameter $\Delta_B \sim \gamma_B k_B T_B$ is expected towards the optimal doping level n_o. For $\gamma_B << \gamma_B^*$, the Eq. (66) can be reduced to the following relation

$$T_B \simeq T_{BEC}^* \left[1 + 1.423\gamma_B \sqrt{k_B T_B^*/\xi_{BA}}\right], \tag{75}$$

where

$$T_{BEC}^* = T_{BEC}\left[1 - n_B V_B(0)/\xi_{BR}\right]. \tag{76}$$

As can be seen from this relation, T_B approaches T_{BEC} when n (or n_B) $\rightarrow n_{c2}$. It is reasonable to assume that, in the overdoped regime, $\tilde{V}_B$ would decrease faster than in the optimally doped region $n_{BCS} < n < n_o$ (where n_{BCS} corresponds to the begining of the strong coupling BCS-like pairing regime) and γ_B becomes almost doping independent for $n > n_o$. Therefore, the decreasing of T_B and Δ_B can be expected for $n > n_o$. The doping dependences of the pairing pseudogap Δ_F and the true SC gap $\Delta_{SC} = \Delta_B$ are schematically summarized in Fig.8, where Δ_F always decreases with increasing doping concentration n, whereas Δ_B first would increase in the doping range $n_{c2} < n < n_o$ and then decreases for $n > n_o$. At $n > n_o$ the decreasing trend of Δ_B is expected to be slower than the exponential decreasing of Δ_F. As a consequence, two curves $\Delta_F(n)$ and $\Delta_B(n)$ would cross at some heavily overdoped level $n = n^* > n_o$ (Fig.8). In underdoped ($n < n_{BCS}$), optimally doped ($n_{BCS} < n < n_o$) and some overdoped ($n_o < n < n^*$) regions, the relationship $\Delta_F > \Delta_B$ can be expected and the vanishing of a SF condensate (or Δ_B) does not lead to the disappearing of bound fermion pairs (or Δ_F). In these doping regions, the SC gap Δ_B should appears inside the pairing pseudogap Δ_F (Fig.7a) as was observed in [15,97-99]. However, at $n > n^*$, the SC gap Δ_B becomes larger than the pairing pseudogap Δ_F (Fig.7b), so that the composite bosons (i.e. Cooper pairs) and their SF condensate disappear simultaneously at the optical and thermal excitation as well as under the magnetic field $H = H_c$. In this case the BCS-like pairing gap Δ_F just as in conventional superconductors serves as the pseudo-SC gap "Δ_{SC}". While the true SC gap Δ_B can be observed in some experiments as the above-gap structure in the heavily overdoped HTSC. The ratio $2\Delta_B/k_B T_B$ increases with increasing n from n_{c2} and slowly tends to the value 2 (see [50]). The doping dependences of the reduced gaps $2\Delta_F/k_B T_F$, $2\Delta_F/k_B T_c$, $2\Delta_B/k_B T_c$ and 2"Δ_{SC}"$/k_B T_c$ are shown in Fig.9. These results are also consistent with various experimental findings [18,72].

6 Formation of the static and dynamic stripe phases

The next key issue is the stripe formation in underdoped HTSC. The solution of this problem may provide a clue to determine the high-T_c mechanism. Various experiments on underdoped and even optimally doped HTSC with $x = 0.06 - 0.12$ have shown [3,17,31-34] that these HTSC exhibit charge-ordered phases or so-called stripe phases which continuously connect the insulating and metallic or SC phases. The nature of the static and dynamic stripes in underdoped HTSC is not fully understood.

We now turn to the stripe formation in the underdoped HTSC. We argue that the competitive localization and delocalization processes of carriers lead to their segregation with the formation of carrier-poor and carrier-rich domains in underdoped HTSC and even in some optimally doped HTSC (when $E_p \geq 0.1eV$). These segregated domains are manifested as the static (i.e. insulating) and dynamic (metallic or SC) stripes. The above results (see Tables 1 and 2) show that the (bi)polaron-induced MIT occurs in the doping range $x_{c2} < x < x_{BCS}$, where the stripe phases intervening between the insulating ($x < x_{c2}$ or $n < n_{c2}$) and metallic ($x > x_{BCS}$) phases are formed. Various experimental results [31-34] indicate that the MIT in LSCO and other HTSC are driven by such stripe formation in the doping range $0.06 \leq x \leq 1/8$. In a dilute polaronic Fermi-gas the Cooper-like pairing leads to the formation of bound polaron pairs with the binding energy

$$\Delta_C = \frac{2(E_{bB} + \hbar\omega)}{\left[exp(1/D_F\tilde{V}_F) - 1\right]}. \tag{77}$$

It is clear that this binding energy of k-space pairs or bipolarons may approach to the binding energy of r-space pairs $E_{bB}+\hbar\omega$ but cannot exceed it. In this case the crossover from k- to r-space pairing regime takes place at $D_F\tilde{V}_F \simeq 0.92$. While, in the strong coupling BCS-like pairing, the binding energy of k-space polaron pairs $2\Delta_F$ may approach also to the effective binding energy of r-space bipolarons $E_{bB} + \hbar\omega$. Then according to (33) the crossover from k- to r-space pairing regime occurs at $D_F\tilde{V}_F \simeq 0.7$. This is often discussed (see [17,27]) as the crossover from the weak-coupling BCS-type superconductivity to the strong-coupling superconductivity described by a BEC of an ideal BG of pre-formed pairs (i.e. r-space pairs). Unlike this conventional crossover scenario our crossover scenario from k- to r-space pairing regime decribes the smooth MIT and it is unrelated to superconductivity. The strong coupling k-space pairing regime is avialable from $D_F\tilde{V}_F \simeq 0.7$ or $n = n_{BCS}$ ($x = x_{BCS}$) to $D_F\tilde{V}_F \simeq 1$ or $n = n_{c2}$ ($x = x_{c2}$). Hence the continuous MIT and the stripe formation are expected for $D_F\tilde{V}_F \simeq 0.7 - 1.0$. The doping dependence of the BCS-like coupling constant has the form $D_F\tilde{V}_F \sim n^{-2/3}$ or $x^{-2/3}$. Then , we find $(x_{c2}/x_{BCS})^{2/3} = D_F\tilde{V}_F = 0.7$ or $x_{BCS} \simeq 1.7x_{c2}$. For $x_{c2} = 0.07$ (see Tables 1,2) we obtain $x_{BCS} \simeq 0.12$ which is very close to the "magic" doping $x = 1/8$ observed in HTSC [31-34]. The BCS-like pairing of polarons occur in the carrier-rich domains, whereas the r-space pairing of polarons takes place in the carrier-poor domains. The bipolaronic insulator(BI)-to-bipolaronic metal (BM) transition in some domains leads to the formation of the metallic (at $T > T_c$) or SC (at $T < T_c$) stripes, while the BM-to-BI transition in other domains leads to the formation of the insulating or static stripes. At $T \to 0$ a MIT is manifested as a superconductor-insulator transition which is driven by boson (i.e. bipolaron) localization but not by fermion localization (cf. [35]). In BSC the formation of static stripes (with immobile r-space bipolarons) at $x < x_{BCS} \simeq 1/8$ is accompanied by the depletion of dynamic stripes (with mobile k-space bipolarons). It leads to the observed suppression of T_c at $x < x_{BCS} = 1/8$ in underdoped HTSC. Above T_F large bipolarons dissociate into two unpaired polarons and polaronic stripes are formed

in the temperature range $T_F < T < T_P$. Above T_P the carriers are quasi-free particles and they are uniformly distributed. So, the self-trapping of carriers due to the strong electron-phonon interactions is responsible for the stripe formation in underdoped HTSC and the strong carrier localization leads to the formation of the (bi)polaronic insulating phases (i.e. static stripes). In this regard, the stripe formation is competing with the pseudogap formation and with the SC phase transition. Recent experimental results [14] speak well for the competitive relationship between the stripe formation and the pseudogap formation.

As can be seen from the above results, the stripe formation is well described on the basis of a large (bi)polaron picture. The nearly small (bi)polarons metalize and become SC carriers at higher doping level. If these polarons have $E_p \geq 0.1eV$, the MIT occurs at $x \geq 0.15$ and the superconductivity driven by the nearly small bipolarons appears also at $x > 0.15$. In a 2d-CuO_2 layer of doped cuprates, the dimer-type small O_2^{2-} bipolarons can be formed with double-well potentials [50]. We believe that such bipolarons may form Bose-glass phase in some HTSC at low temperature. Apparently, the Bose-glass phase observed in LSCO is caused by the off-center configurations of small O_2^{2-} bipolarons.

7 Generic and relevant electronic phase diagrams

The puzzling normal and SC states of doped HTSC and all their anomalous properties can be understood properly in terms of the generic and relevant temperature-doping ($T - x$) phase diagrams. Many theoretical [10,17,46,50,51,74,75,79] and experimental [2,7-9,11,14,27,39,69] $T - x$ phase diagrams have been proposed. However, general consensus on $T - x$ phase diagrams of doped HTSC has not yet emerged. So, the problem of the generic and relevant $T - x$ phase diagrams is still unresolved. The rich $T - x$ phase diagrams which are observed in different experiments, should be accounted for by any consistent theory. We discuss the $T - x$ phase diagrams of doped HTSC within the above developed theory of large (bi)polarons and the FBL theory of novel superconductivity. The above presented theory of impurity (or defect) centers and large r-space (bi)polarons predicts the existence possibility of the AF insulator phase below T_N, (for $x < x_{c1}$), the bipolaronic insulator phase below $T_F \simeq E_{bB}/k_B$ (for $x < x_{c2}$), polaronic insulator phase below $T_P \simeq E_p/k_B$ (for $x < x_{c2}$) and ordinary metallic phase above T_P. At $x < x_{c2}$ the crossover temperatures T_P and T_F are nearly doping independent. The superconductivity appears at $x > x_{c2}$ and the above two distinct FBL scenarios lead to the nearly inverse-parabolic doping dependence of T_c [50] (cf. experimental results [2,8,9,14,72,110]). As the SF condensation temperature T_B first increases nearly as $\sim n_B^{2/3}$ (for a 3d-BG) and $\sim n_B$ (for a 2d-BG) and goes through a maximum at $n = n_o$ and then decreases at $n > n_o$ [50]. While, the crossover temperatures T_P and T_F would always decrease with increasing n (or x) from n_{c2} (or x_{c2}). We believe that the polarons in doped HTSC can be formed with slightly different E_p due to the structure inhomogeneities with different ε_∞ and ε_0. Therefore, at $E_p \leq 0.07eV$ the

three curves $T_P(x)$, $T_F(x)$ and $T_B(x)$ in $T-x$ phase diagram of LSCO can cross near $x = x_o$. Then the polaronic quantum critical point $x_p \simeq 0.20$ corresponding to the polaronic metal (PM)-to-normal metal transition lies hidden (see Fig.10a) under the SC transition temperature T_c. While, at $E_p > 0.07eV$ the upper curve $T_P(x)$ crossing the lower curve $T_F(x)$ in the heavily overdoped region (Fig.10b) and ending in the polaronic quantum critical point $x_p \simeq 0.24$ lies away from x_o. The above physical picture seems to be relevant and characteristic for other doped cuprates. Two generic and relevant $T-x$ phase diagrams of LSCO obtained by us on the basis of the above large (bi)polaron formation scenarios are presented in Fig.10. These results are fully consistent with experimental findings [2,11,14,16,17,39,72].

8 Conclusions

We have demonstrated that the understanding of the unusual normal and SC state properties of doped HTSC requires the novel theoretical approaches combining strong coupling, normal-state pairing and true SF condensation effects, 3d properties and going beyond the scope of the conventional Mott-Hubbard band formalism, Landau Fermi-liquid model, BCS-like pairing model of carriers (at T_c) and BEC model of an ideal BG of r-space pairs. In particular, we have shown that the strong electron-phonon interactions or (bi)polaronic effects, which without any doubt are present in these materials, determine the basic trends of the formation of anomalous insulating and metallic states in lightly doped, underdoped, optimally doped and even overdoped HTSC. The continuum theory of extrinsic and intrinsic carrier self-trapping has been employed to examine the electronic states of the doped holes in HTSC. Our calculations show that in LSCO and other doped HTSC the hydrogen-like impurity (or defect) centers with trapped carriers can be formed due to the suppression of the carrier-phonon interactions near the impurity (or defect) by the short-range defect potential. As the temperature and doping are increased, the ionization of these impurity (or defect) centers occur and the liberated carriers are self-trapped immediately in a deformable lattice with the formation of r-space large D or nearly small L (bi)polarons due to the strong short- and long-range carrier-lattice interactions between the impurity sites. We have found that in lightly doped HTSC (i.e. $x_{c1} < x < x_{c2}$) the PI and BI states are formed below the characteristic crossover temperatures T_P and T_F, respectively. At very low doping level ($x < x_{c1}$) these (bi)polaronic insulating states are formed above the Neel temperature (Fig.10). The novel insulating states of lightly doped HTSC can be understood properly within the large D (bi)polaron model. It is reasonable to assume that the large D polarons form a superlattice as x increares to x_{c2} and the (bi)polaronic mechanism for the MIT can take place in LSCO and other hole-doped HTSC at the overlapping of the in-gap polaronic band with the valence band. We have obtained the proper criterion for the MIT within the large D (bi)polaron model. As x moves through x_{c2} the (bi)polaronic insulating states evolve into the BM and PM states in the underdoped ($x_{c2} < x < x_{BCS}$) and optimally doped ($x_{BCS} < x < x_o$)

regions as well as the (bi)polaronic insulating gaps evolve into the large polaronic and small bipolaronic pseudogaps in the excitation spectrum of HTSC. We have demonstrated that these two (bi)polaronic pseudogaps opening in the normal state of underdoped and optimally doped HTSC at the crossover temperatures T_P and T_F above T_c are observed as the large and small pseudogaps in the excitation spectrum of these HTSC in different experiments above T_c. Our quantitative analysis are carried out on the basis of the FBL model. We have found that the small BCS-like pairing pseudogap exist above T_c only in underdoped and optimally doped HTSC but the large non-pairing polaronic pseudogap can exist even in some overdoped HTSC (Fig.10). Unlike the conventional superconductors, the underdoped and optimally doped HTSC have three types of metallic states above T_c: (i) ordinary gapless metallic state (above T_P); (ii) pseudogapped polaronic (below T_P) and (iii) pseudogapped bipolaronic (below T_F) metallic states. Therefore, the anomalous metallic properties of these materials above T_c are consistently explained in terms of the (bi)polaronic pseudogap phenomena which are descibed by the novel FBL theory [50,51]. The FBL model predicts the existence of a degenerate polaronic Fermi-gas (in the temperature range $T_F < T < T_P$) and a non-degenerate bipolaronic BG (in the temperature range $T_c < T < T_F$) in underdoped and optimally doped HTSC. The anomalous optical, transport, magnetic and other physical properties of these HTSC observed in the normal state result from the formation of the polaronic pseudogap (below T_P) and the BCS-like pairing (bipolaronic) pseudogap (below T_F). We argue that the large r- and k-space (bi)polarons as well as quasi-free carriers and cooperons are relevant carriers in doped HTSC. In Fermi systems, first the BCS-like (s-, p- and d-wave) pairing of carriers above T_c or at T_c leads to the formation of two-fermion composite bosons (cooperons and bipolarons) and then the successive transitions of these bosons to the SF states at PC below $T_c = T_B$ and SPC below $T = T_B^* < T_c$ lead to the formation of the true SC states. These successive BCS-like second-order transition (at $T_F \geq T_c$) (for which there is experimental evidence in [111] with $T_F = 229K$) and second-order SF transition (at $T_c = T_B$) and first-order SF transition (at $T_B^* < T_B$) are described by the two-stage FBL model of novel superconductivity. So, the novel superconductivity results from the coexistence of two distinct order parameters Δ_F and Δ_B, characterizing attracting fermion pairs and composite boson pairs, respectively. The coexistence of the order parameters Δ_F and Δ_B leads to the novel superconductivity by two FBL scenarios. One of these scenarios is realized in so-called FSC and the other takes place in BSC. As discussed above, the pairing pseudogap Δ_F and the SC gap Δ_B have quite different origins. This is confirmed now experimentally [15,18,97-99]. The doping dependences of Δ_F and Δ_B are also quite different and these distinctive doping dependences of the pairing pseudogap and the SC gap are consistent well with the experimental results [18]. There is no any anomaly below T_F in the temperature dependence of the BCS-like order parameter Δ_F. In contrast, for $\gamma_B \ll \gamma_B^*$ the temperature dependence of the SC order parameter Δ_B has strongly pronounced kink-like feature at $T_B^* < T_B = T_c$. Such a feature of the SC order parameter and first-order SC phase transition can be observed experimentally in BSC

(i.e. underdoped and optimally doped HTSC). So far, the first-order SC phase transition was observed in some experiments [40-42]. We have shown that the non-zero DOS in the BCS-like pairing gap Δ_F and in the bottom of this gap observed as the ZBCP and low-bias conductance peak are caused by the absence of the low-energy gap Δ_{SF} in the excitation spectrum of a 3d-SF Bose-liquid and by the presence of the another low-energy SC gap Δ_B inside the small pairing pseudogap Δ_F. As we have discussed before [50], various experiments speak well for two distinct SC transitions at $T_{c1} = T_B$ and $T_{c2} = T_B^*$, two λ-like jumps of the specific heat and two lines which intersect both the $H_{c1}(T)$ and the $H_{c2}(T)$ curve at some characteristic temperature or upward curvature (or kink-like features) of the $H_{c1}(T)$ and $H_{c2}(T)$ below T_c (see [50]). The above experimental results have provided evidences for the validity of the two-stage FBL theory (in particular, the theory of fluctuationless BCS-like pairing of carriers above T_c and the theory of SF condensation of attracting composite bosons) and the 3d-superconductivity in doped HTSC. With descreasing γ_B from γ_B^*, the temperature T_B^* of the first-order SPC–PC of attracting composite bosons shifts towards $T_B = T_c$ and the splitting of the SC (or SF) phase transition decreases and becomes impossible to observe at $\gamma_B \ll 1$ (e.g. in conventional superconductors and overdoped HTSC). Such a shifting of two SC (or SF) transition temperatures T_{c1} and T_{c2} towards each other with increasing x from x_o can be also observed in HTSC (with 3d composite bosons) just as it was observed in heavy-fermion superconductors (under the magnetic field) [106] and in ^3He (at decreasing of the pressure) [96]. In contrast, in HTSC with 2d composite bosons and $T_B^* = 0$ the second SC phase transition at $T_{c2} \neq 0$ is absent. As in this case the SPC of attracting 2d composite bosons is possible only at $T = T_B^* = 0$, while the PC of these bosons takes place in the temperature range $0 < T \leq T_B = T_c$. The PC of attracting 3d- and especially 2d composite bosons should be manifested as the half-integer $\hbar/4e$ magnetic flux quantization in HTSC. So far, the magnetic flux quantum $\hbar/4e$ was observed in the grain boundaries and in thin films of some HTSC. Such a magnetic flux quantum can be also observed in 3d region of doped HTSC by using the sensitive experimental methods.

We discussed the stripe formation in the underdoped HTSC ($x_{c2} < x < x_{BCS}$) on the basis of the large D (bi)polaron model and the strong coupling BCS-like pairing model of such D polarons. It is found that the formation of the static stripes is associated with the formation of large r-space immobile (bi)polarons at $x \leq x_{BCS} = 1/8$ and the suppression of T_c is caused by the depletion of the dynamic stripes containing mobile large D (bi)polarons.

We have obtained the generic and relevant $T - x$ phase diagrams of HTSC on the basis of the large (bi)polaron formation scenarios. The possible changes of the crossover temperatures (T_P, T_F and T_c) and quantum critical points ($x_{c1}, x_{c2}, x_{BCS}, x_o$ and x_p) in these phase diagrams as a function of the binding energies of large D (bi)polarons are discussed. We have shown that $T - x$ phase diagrams and possible crossover temperatures and quantum critical points in these phase diagrams are consistent with the existing experimental $T - x$ phase diagrams. We believe the theory presented here based on the continuum model of extrinsic and intrinsic carrier self-

trapping, tight-binding models and the novel two-stage FBL model of superconductivity is the consistent and adequate approach to the problem of the normal and SC states of doped HTSC. This theory explains without any difficulty a wide variety of phenomena and may provide a clear and complete understanding of the basic normal and SC state properties of HTSC in the lightly doped, underdoped, optimally doped and overdoped regions.

Finally, we summarize key results and formulate the basic principles of the theory of novel normal and SC states in doped HTSC as follows.

1. The strong electron-phonon interactions are the characteristic for doped HTSC and other oxides and they are the main driving forces for the formation of the novel insulating, metallic and SC states in these materials.

2. Large (bi)polarons are the relevent carriers in underdoped, optimally doped and some overdoped HTSC with $\varepsilon_\infty/\varepsilon_0 \leq 0.1$, while quasi-free carriers and cooperons exist in overdoped HTSC.

3. The insulating state of doped HTSC is determined by the (bi)polaronic energy gaps and not by the Mott-Hubbard gap.

4. The metal-insulator transition in doped HTSC is the new (bi)polaron (i.e. electron-phonon)-induced metal-insulator transition and not correlation-induced Mott transition.

5. The large polaronic and small BCS-like pairing (bipolaronic) pseudogaps exist in the excitation spectrum of underdoped and optimally doped HTSC both above T_c and below T_c, while the large polaronic pseudogap can exist in some overdoped HTSC, where the binding energy E_p of large polarons larger than $0.07eV$.

6. The polaronic quantum critical point between the Landau and non-Landau Fermi-liquid states exists in LSCO at the doping level $x_p \leq 0.20$ (for $E_p < 0.07eV$) or $x > 0.20$ (for $E_p \geq 0.07eV$) at which the large polaronic pseudogap temperature T_P falls to zero within the SC region of the $T - x$ phase diagrams.

7. Both the polaronic pseudogap and the BCS-like pairing pseudogap (opening simultaneously in the charge and spin channels) is not a precursor to the SC gap. The BCS-like pairing pseudogap and the SC gap have quite different origins (or symmetries) and they are related to different phenomena (i.e. BCS-like pairing of carriers and SF condensation of two-fermion composite bosons).

8. The novel superconductivity in any Fermi systems results from the coexistence of the BCS-like pairing pseudogap and the true SC gap. There the emerging of superconductivity is possible at the SF single particle and pair condensation of attracting composite bosons (i.e. bipolarons and cooperons) but not at the pairing of carriers (electrons or holes).

9. The SF single particle and pair condensation of attracting composite bosons leading to the formation of two novel SC (or SF) states are quite different from the conventional BEC of an ideal Bose-gas.

10. The superconductivity (or superfluidity) is peculiar only to a Bose-liquid but not to a

Fermi-liquid and to an ideal Bose-gas.

Acknowledgments

The author would like to thank the Condensed Matter Group and in particular Prof. Yu Lu for hospitality at the Abdus Salam ICTP. This work was supported in part by grant No. 12-00 Fundamental Research Foundation of Uzbek Academy of Sciences.

References

[1] J.G. Bednortz, K.A. Muller. Z.Phys. B64, 189 (1986).

[2] R.J. Birgeneu, G. Shirane, in Physical properties of High Temperature superconductors I, edited by D.M. Ginsberg (Mir, Moscow, 1990) Chap. 4; P.B. Allen, Z. Fisk, A. Migliori, ibid., Chap. 5; J.T. Markert, Y. Dalichaouch, M.B. Maple, ibid., Chap. 6; Th. Timusk, D.B. Tanner, ibid., Chap. 7.

[3] J. Fink et al., Physica C185-189, 45 (1991).

[4] A. Fujimori, H. Namatane, Physica C185-189, 51 (1991).

[5] Z. Schlesinger, et al., Physica C235-240, 49 (1994).

[6] Ch. Renner, O. Fischer, Physica C235-240, 53 (1994).

[7] B. Batlogg, et al., Physica C235-240, 130 (1994).

[8] H. Ding, et al., Nature 382, 51 (1996).

[9] A.G. Loeser, et al., Science 273, 325 (1996).

[10] P.W. Anderson, The Theory of superconductivity in the High-T_c Cuprate Superconductors (PrincetonUniversity Press, Princton, 1997).

[11] B. Batlogg, Physica C282-287, xxiv (1997); B. Batlogg, C. Varma. Phys. World. February, 33 (2000).

[12] G.V.M. Williams et al., Phys. Rev. B58, 15053 (1998-II).

[13] C.C. Tsuei, J.R. Kirtley, Physica C282-287, 4 (1997).

[14] S. Uchida, Physica C282-287, 12 (1997); Physica C 341-348, 823 (2000).

[15] G. Ruani, P. Ricci, Phys.Rev. B55, 93 (1997-I).

[16] M.A. Kastner et al., Rev.Mod.Phys. 70, 897 (1998).

[17] M. Imada et al., Rev.Mod.Phys. 70, 1039 (1998).

[18] G. Deutscher, Nature 397, 410 (1999).

[19] E.E. Alp, G.K. Shenoy, D.G. Hinks et al., Phys.Rev. B35, 7199 (1987).

[20] P.V. Avramov, S.G. Ovchinnikov, Fiz.Tverd.Tela 42, 770 (2000).

[21] N. Bulut, D.J. Scalapino, S.R. White, Phys. Rev. B47, 6157 (1993); Phys. Rev. B50, 9623 (1994).

[22] E. Dagotto, Rev. Mod. Phys. 66, 763 (1994).

[23] J.R. Schieffer, X.G. Wen, S.C. Zhang, Phys.Rev.B39, 11663 (1989).

[24] B.K. Chakraverty et al., J. Less-Common Metals. 150, 11 (1989).

[25] D. Emin, M.S. Hillery, Phys.Rev. B39, 6575 (1989).

[26] A.S. Alexandrov, N.F. Mott, Int.J.Mod.Phys. B8, 2075 (1994).

[27] Y.J. Uemura, Physica C282-287, 194 (1997)

[28] G. Baskaran, E. Tosatti, L. Yu, Int.J.Mod.Phys. B1, 555 (1988).

[29] X. Dai, Zh.-B. Su, L. Yu, Phys.Rev. B56, 5583 (1997-I).

[30] J. Lorenzana, L.Yu, Mod.Phys.Lett. B5, 1515 (1991).

[31] B.G. Levi, Physics Today, June, 19 (1998).

[32] B. Nachumi et al., Phys.Rev. B58, 8760 (1998-I).

[33] J. Zaanen, O.Y. Osman, W.van Saarloos, Phys.Rev. B58, R11868 (1998-II).

[34] J.L. Cohn et al., Phys.Rev. B59, 3823 (1999-I).

[35] A.M. Goldman, N. Markovic, Physics Today. November, 39 (1998).

[36] J.M. Harris et al., Phys.Rev. B54, R15665 (1996-II).

[37] Ch. Renner et al., Phys. Rev Lett. 80, 149 (1998).

[38] N. Miyakawa et al., Phys.Rev.Lett. 80, 157 (1998).

[39] T. Timusk, B. Statt, Rep. Prog. Phys. 62,61 (1999).

[40] J.M. Barbut et al., Physica C235-240, 2855 (1994).

[41] T. Ishida et al., Phys.Rev. B58, 5222 (1998-I); A. Bianccni et al., Physica C341-348, 1719 (2000).

[42] M.T. Beal-Monod, Phys,Rev. B58, 8830 (1998-I).

[43] Ch. Renner, O. Fischer, Physica C 235-240, 53 (1994).

[44] K. Kitazawa, Science. 271, 261 (1996); M.B. Walker, P. Pairor, Physica C 341-348, 1523 (2000).

[45] A. Ino et al., Phys.Rev.Lett. 81, 2124 (1998); T. Sato et al., Physica C 341-348, 815 (2000); A. Fujimori et al., Physica C 341-348, 2067 (2000).

[46] J. Schmalin, D. Pines, B. Stojkovic, Phys.Rev. B60, 667 (1999-I).

[47] A. Lanzara et al Nature 412, 510 (2001).

[48] S. Dzhumanov, A.A. Baratov, S. Abboudy, Phys.Rev. B54, 13121 (1996-II).

[49] S. Dzhumanov, A.A. Baratov, Superlattices and Microstructures. 21, Suppl.A, 265 (1997).

[50] S. Dzhumanov, Physica C235-240, 2269 (1994); Int.J.Mod.Phys. B12, 2151 (1998).

[51] S. Dzhumanov, Solid State Commun. 115, 155 (2000); Physica C 341-348, 159 (2000).

[52] Y. Toyozawa, Physica B116, 7 (1983).

[53] S. Dzhumanov, P.K. Khabibullaev, Izv. Akad. Nauk Uzb. SSR. Ser. Fiz. Math. Nauk. 1, 47 (1990).

[54] A.R. Bishop et al., Z.Phys. B76, 17 (1989).

[55] V.I. Belinicher, A.L. Chernyshev, L.V. Popovich, Physica C235-240, 2183 (1994).

[56] S. Dzhumanov, A.A. Baratov, Uzb. Dokl. Akad. Nauk. 4, 16 (1995).

[57] G. Verbist, F.M. Peeters, J.T. Devreese. Physica Scripta. T39, 66, (1991).

[58] M. Weger, L. Burlachkov, Physica C235-240, 2387 (1994).

[59] S.V. Varyukhin, A.A. Zakharov, Physica C185-189, 975 (1991).

[60] N.F. Mott, E.A. Davis, Electronic processes in Noncrystalline Materials (Mir, Moscow, 1974).

[61] S. Sugai, Physica C185-189, 76 (1991).

[62] B.K. Ridly, Quantum Processes in Semiconductors (Mir, Moscow, 1986).

[63] Ch. Lushchik et al., Trudy Inst. Fiz. AN Est. SSR. 63, 137 (1989).

[64] J.P. Lu, Q. Si, Phys.Rev. B42, 950 (1990).

[65] M. Hiraa, T. Uda, Y. Murayama, Physica C185-189, 1551 (1991).

[66] R.C. Baetzold, Phys.Rev. B42, 56 (1990).

[67] V. Cataudella, G. Iadonisi, D. Ninno, Physica Scripta. T39, 71 (1991); Europhys.Lett. 27, 709 (1992).

[68] V.D. Lakhno, Phys.Rev. B51, 3512 (1995).

[69] D. Mihailovic, T. Mertelj, K.A. Muller, Phys.Rev. B57, 6116 (1998-II).

[70] T.H.H. Vuong, D.C. Tsui, V.G. Goldman, Solid State Commun. 63, 525 (1987).

[71] A.S. Alexandrov, V.V. Kabanov, D.K. Ray, Physica C235-240, 2365 (1994).

[72] T. Nakano et al., J. Phys. Soc. Jpn. 67, 2622 (1998).

[73] Y. Yanase, K. Yamada, J. Phys. Sos. Jpn. 68, 548 (1999); ibid., P.2999.

[74] G. Kotliar, J. Liu. Phys.Rev. B38, 5142 (1988); P.A. Lee, N. Magaosa, Phys. Rev. B 46, 5621 (1992).

[75] T. Tanamoto, K. Kohno, H. Fukuyama, J. Phys. Soc. Jpn. 61, 1886 (1992); H. Fukuyama, H. Kohno, Physica C 282-287, 124 (1997).

[76] J.R. Schriffer, A.P. Kampf, J.Phys.Chem. Solids. 56, 1673 (1995).

[77] J. Friedel, J. Phys.; Condens. Matter. 1, 7757 (1989).

[78] S. Doniach, M. Inui, Phys. Rev. B41, 6668 (1990).

[79] V.J. Emery, S. Kivelson, Nature. 374, 434 (1995).

[80] B. Janko, J. Maly, K. Levin, Phys.Rev. B56, R11407 (1997); M. Randerira, cond.-mat./9710223.

[81] J.G. Naeini et al., Phys.Rev. B57, R11077 (1998-II).

[82] C. Panagopoulos et al., Phys.Rev. B60, 14617 (1999-I); T. Shibauchi et al., Phys. Rev. Lett. 86, 5763 (2001)..

[83] H.Y. Hwang et al., Phys. Rev. Lett. 72, 2636 (1994).

[84] J.L. Tallon, J.W. Loram, Physica C 349, 53 (2001).

[85] A.S. Alexandrov, Physica C 341-348, 107 (2000).

[86] J.-S. Zhou, J.B. Goodenough, H. Sato, M. Naito, Phys. Rev. B59, 3872 (1999-I).

[87] L.G. Gomersall, B.L. Gyorffy. Phys. Rev. Lett. 33, 21, 1286 (1974). M.N. Mikheeva et al., Fiz. Tverd. Tela. 42,2113 (2000).

[88] K. Kawabata et al., Phys.Rev. B58, 2458 (1998-I); I. Iguchi et al., Nature 412, 420 (2001).

[89] R.Smith. Semiconductors (Mir, Moscow, 1982).

[90] S. Uchida, Physica C 341-348, 823 (2000); H. Sato et al., Physica C 341-348, 1767 (2000).

[91] A.I Romanenko et al., Physica C 282-287, 1157 (1997).

[92] M.J. Rice, Y.R. Wang, Phys. Rev. B37, 5893 (1988).

[93] J.M. Wheatly, T.C. Hsu, P.W. Anderson, Phys.Rev. B37,5897 (1988)

[94] E.A. Lynton, Superconductivity (Mir, Moscow, 1971)

[95] A. Vaknin, Z. Ovadyahu, J. Phys.: Condens. Matter. 9, L303 (1997)

[96] D.M. Lee, Rev.MOd. Phys. 69, 645 (1997); D.D. Osheroff, ibid., P.667; R.C. Richardson, ibid., P.683.

[97] M. Suzuki, S. Karimoto, K. Namekawa, J.Phys. Soc.Jpn. 67, 732 (1998)

[98] V.M. Krasnov et al., Phys. Rev. Lett. 84, 5860 (2000).

[99] V.M. Svistunov et al., Pis'ma v ZhETF. 71, 418 (2000).

[100] J. Ranninger, S. Robaszkiewicz, Physica B135,468 (1185)

[101] R. Friedberg, T.D. Lee. Phys. Lett. A138, 423 (1989)

[102] W.A.B. Evans, Y.Imry, Nuovo Cim. B 63, 155 (1969)

[103] T. Oki et al., Physica C 353, 213 (2001).

[104] G. Deutscher et al., Physica C 341-348, 1629 (2000); H.-W. Cheng et al., Physica C 341-348, 2159 (2000).

[105] I. Shigeta et al., J. Phys. Sos. Jpn. 69, 2743 (2000).

[106] R.A. Fisher et al., Phys. Rev. Lett. 62, 1411 (1989); R. Joynt, Physica C 162-164, 1673 (1989).

[107] V.V. Moshcholkov et al., Physica C 235-240, 2513 (1994); A. Sidorenko et al., Physica C 235-240, 2615 (1994); A. Schilling et al., Physica C 235-240, 2741 (1994).

[108] A. Dorosinskii et al., Physica C 235-240, 2727 (1994); V.V Metlushko et al., Physica C 235-240, 2793 (1994).

[109] P.J. Baimatov, Ph. D. Thesis (Tashkent, 1995)

[110] C.N.R. Rao, A.K. Ganguli, Physica C 235-240, 9 (1994)

[111] K. Fossheim et al., Int. J. Mod. Phys. B1, 1171 (1988).

FIGURE CAPTIONS

1. The doping dependences of the BCS-like pairing pseudogap temperature T_F in LSCO.

2. The temperature dependences of the high-energy polaronic and low-energy BCS-like pseudogaps: (a) for underdoped and optimally doped HTSC and (b) for overdoped HTSC.

3. The temperature dependence of the resistivity of optimally doped HTSC.

4. The temperature dependence of the magnetic susceptibility of underdoped and optimally doped HTSC.

5. The temperature dependences of $\tilde{\mu}_B$ and Δ_B at $\gamma_B > \gamma_B^*$: (a) for a 3d- BG and (b) for a 2d- BG.

6. The temperature dependences of $\tilde{\mu}_B$ and Δ_B for a 3d- BG: (a) at $\gamma_B < \gamma_B^*$ and (b) at $\gamma_b << \gamma_B^*$.

7. The temperature dependences of the pairing pseudogap Δ_F and the true SC gap Δ_B: (a) for underdoped and optimally doped HTSC; and (b) for heavily overdoped HTSC.

8. The doping dependences of the pairing pseudogap and the true SC gap in HTSC.

9. The doping dependences of the reduced pseudogaps $2\Delta_F/k_BT_F$, $2\Delta_F/k_BT_c$, SC gap $2\Delta_B/k_BT_c$ and BCS-like pseudo SC gap 2"Δ_{SC}/k_BT_c in HTSC.

10. The generic and relevant $T-x$ phase diagrams of LSCO determined from the formation scenarios of large (bi)polarons: (a) for $E_p < 0.07eV$ and (b) $E_p > 0.07eV$.

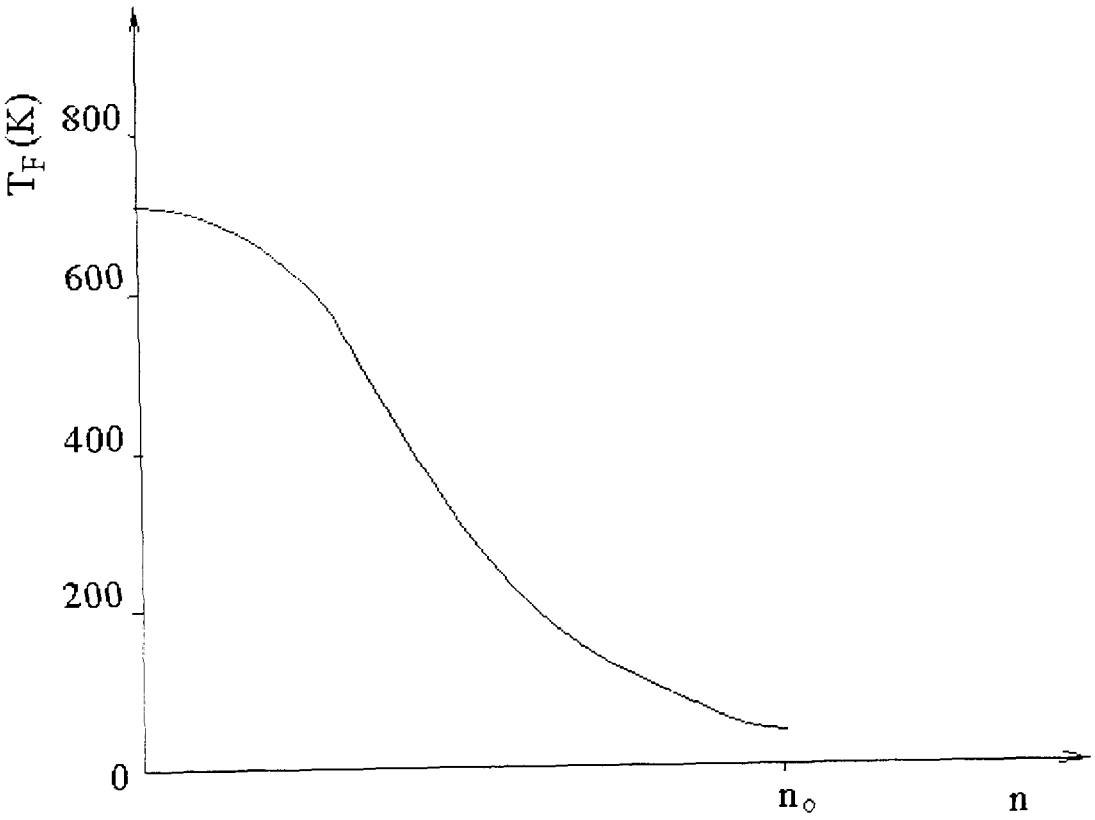

Fig. 1

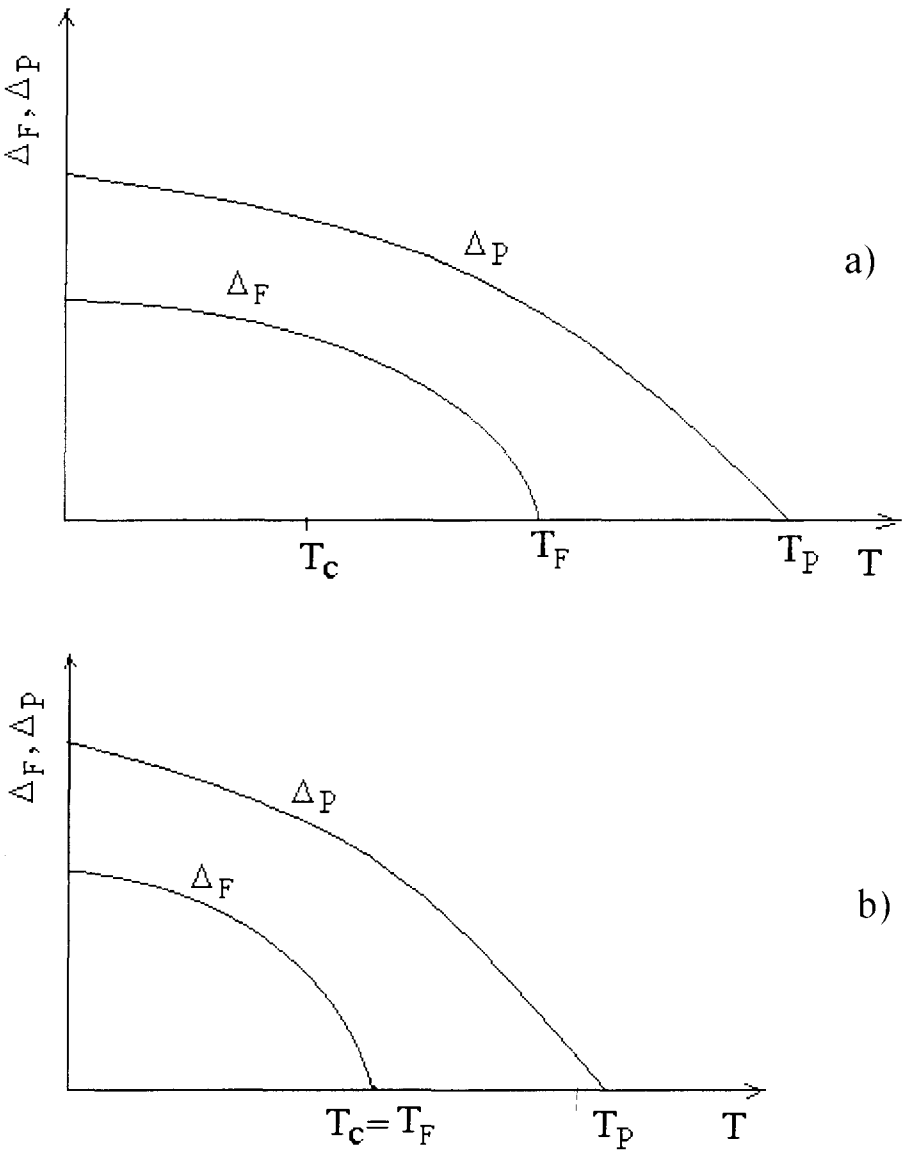
Δ_F, Δ_P
Δ_P
Δ_F
a)
T_c
T_F
T_P
T
Δ_F, Δ_P
Δ_P
Δ_F
b)
$T_c = T_F$
T_P
T

Fig. 2

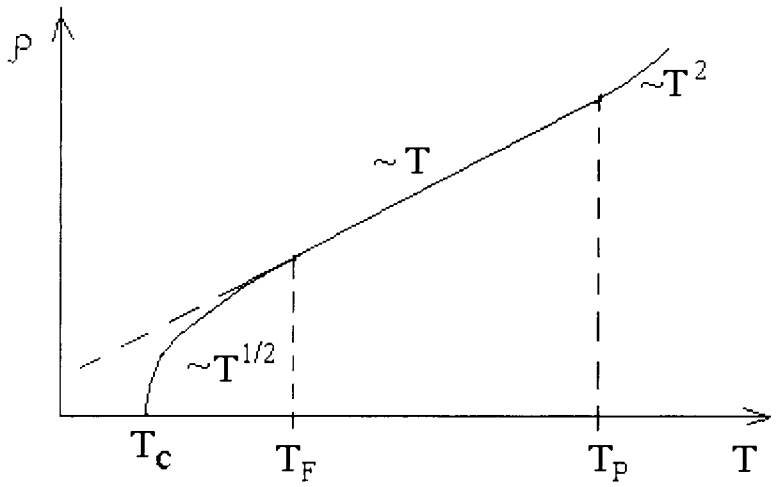

Fig. 3

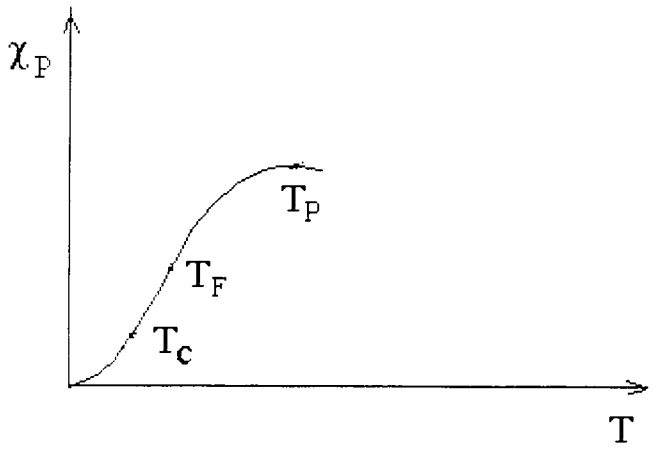

Fig. 4

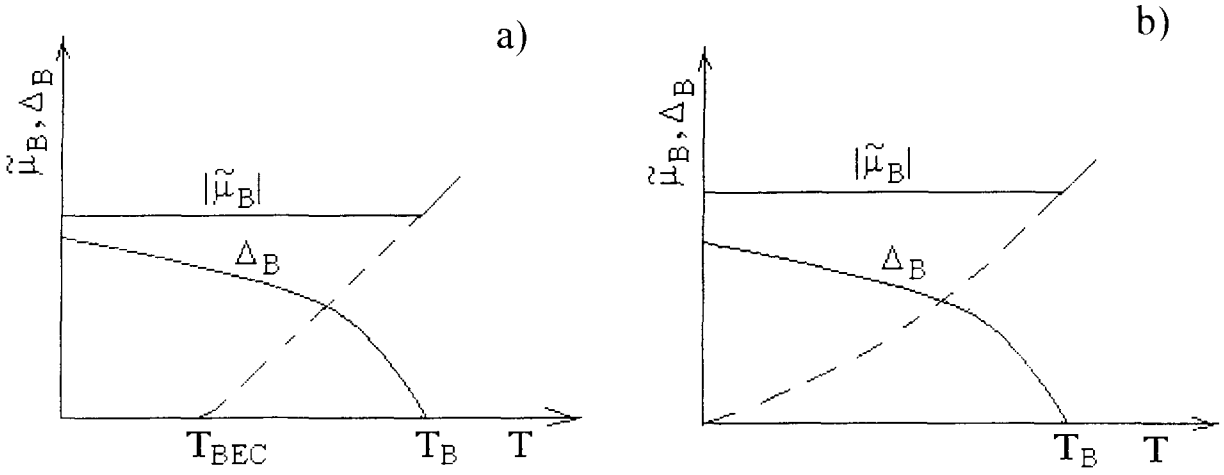
a)
b)
$\tilde{\mu}_B, \Delta_B$
$|\tilde{\mu}_B|$
Δ_B
T_{BEC}
T_B
T

Fig. 5

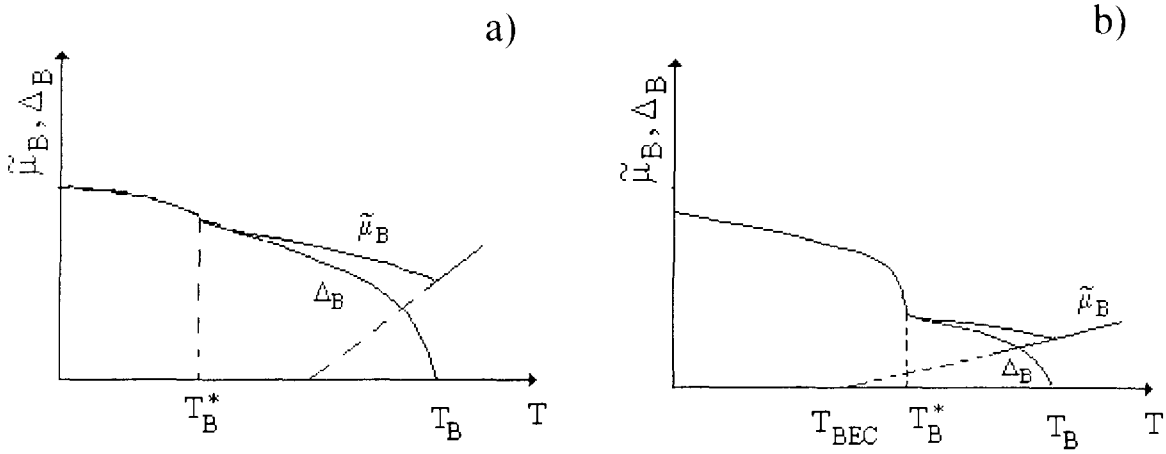
a)
b)
$\tilde{\mu}_B, \Delta_B$
$\tilde{\mu}_B$
Δ_B
T_B^*
T_{BEC}
T_B
T

Fig. 6

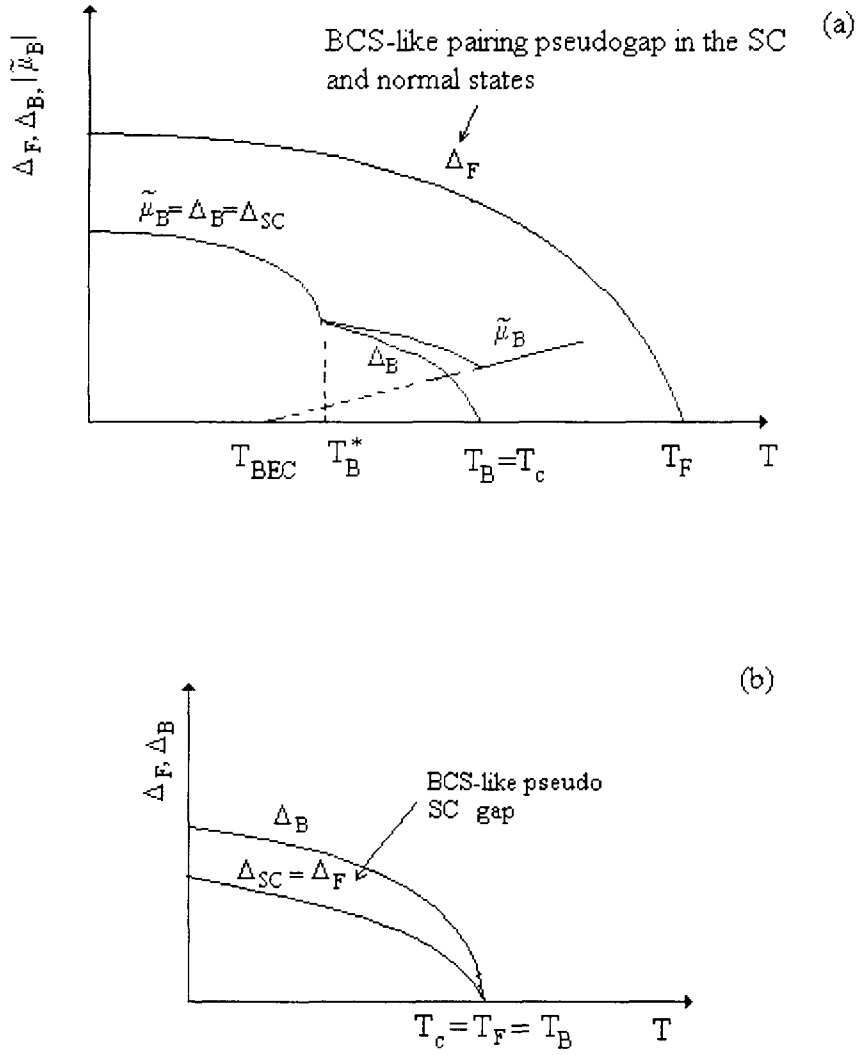
(a)
BCS-like pairing pseudogap in the SC and normal states
$\Delta_F, \Delta_B, |\tilde{\mu}_B|$
Δ_F
$\tilde{\mu}_B = \Delta_B = \Delta_{SC}$
$\tilde{\mu}_B$
Δ_B
T_{BEC}
T_B^*
$T_B = T_c$
T_F
T
(b)
Δ_F, Δ_B
BCS-like pseudo SC gap
Δ_B
$\Delta_{SC} = \Delta_F$
$T_c = T_F = T_B$
T

Fig. 7

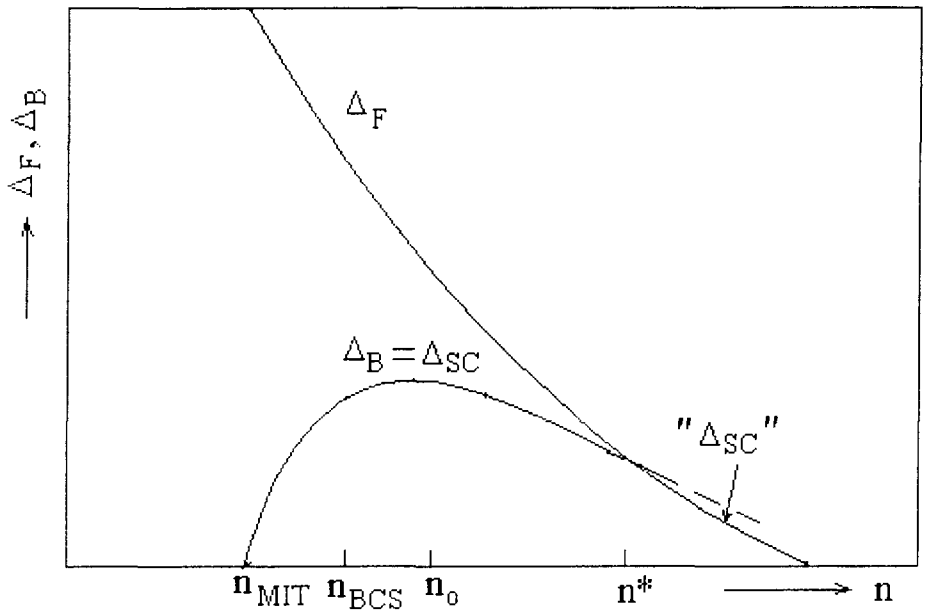
Δ_F, Δ_B
Δ_F
$\Delta_B = \Delta_{SC}$
"Δ_{SC}"
n_{MIT}
n_{BCS}
n_0
n*
n

Fig. 8

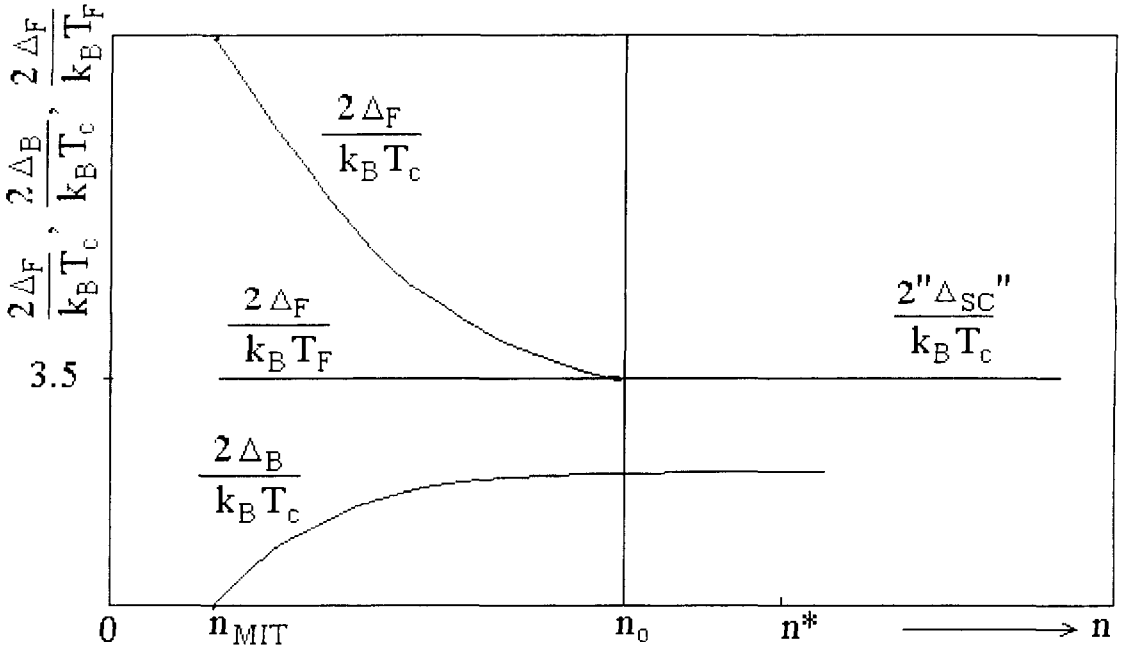
$\frac{2\Delta_F}{k_B T_c}, \frac{2\Delta_B}{k_B T_c}, \frac{2\Delta_F}{k_B T_F}$
$\frac{2\Delta_F}{k_B T_c}$
$\frac{2\Delta_F}{k_B T_F}$
3.5
$\frac{2''\Delta_{SC}''}{k_B T_c}$
$\frac{2\Delta_B}{k_B T_c}$
0
n_{MIT}
n_0
n*
n

Fig. 9

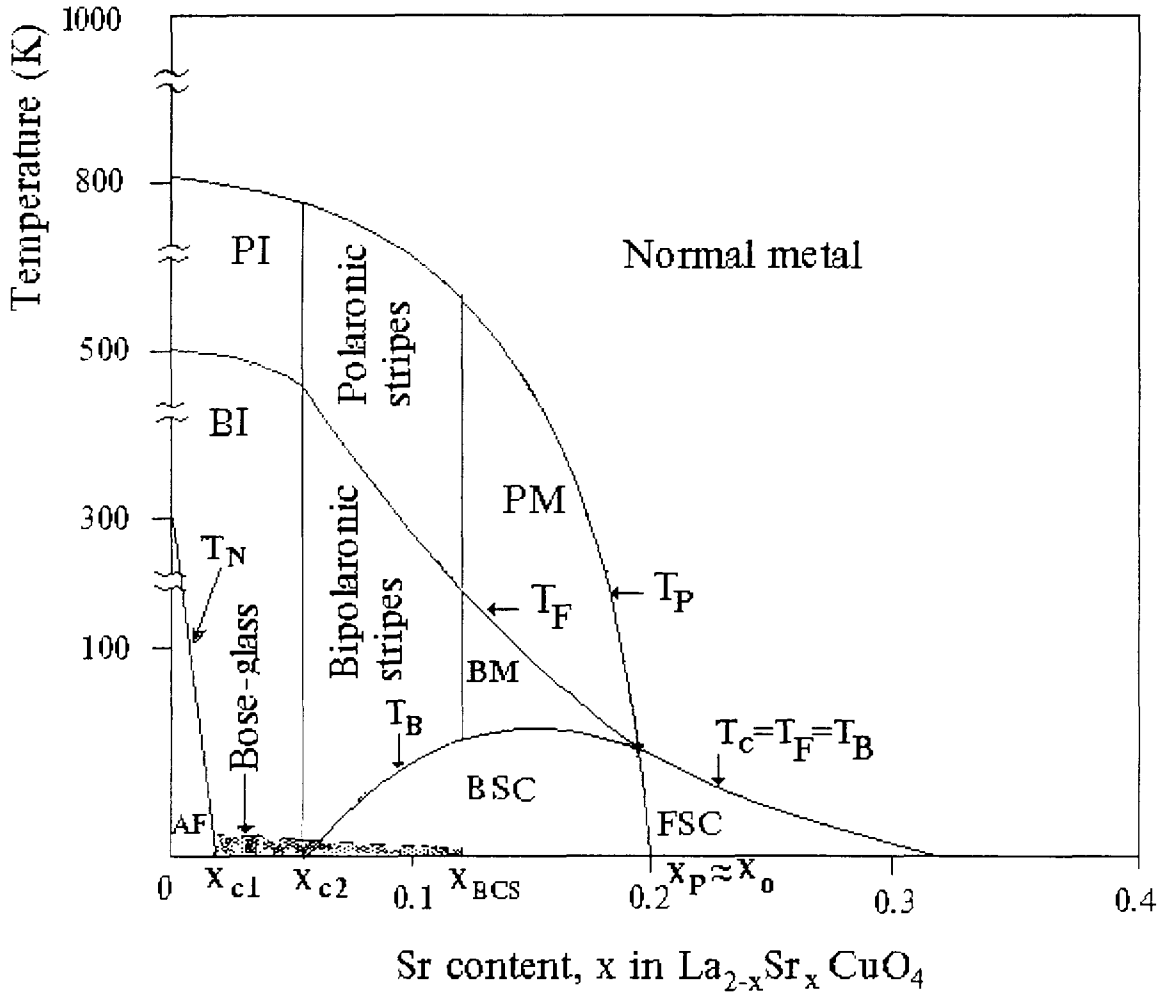
Temperature (K)
1000
800
500
300
100
PI
BI
Normal metal
Polaronic stripes
Bipolaronic stripes
PM
T_N
T_F
T_P
T_B
BM
$T_c=T_F=T_B$
BSC
FSC
AF
Bose-glass
0
x_{c1}
x_{c2}
0.1
x_{BCS}
0.2
$x_P \approx x_0$
0.3
0.4
Sr content, x in $La_{2-x}Sr_xCuO_4$

Fig. 10a

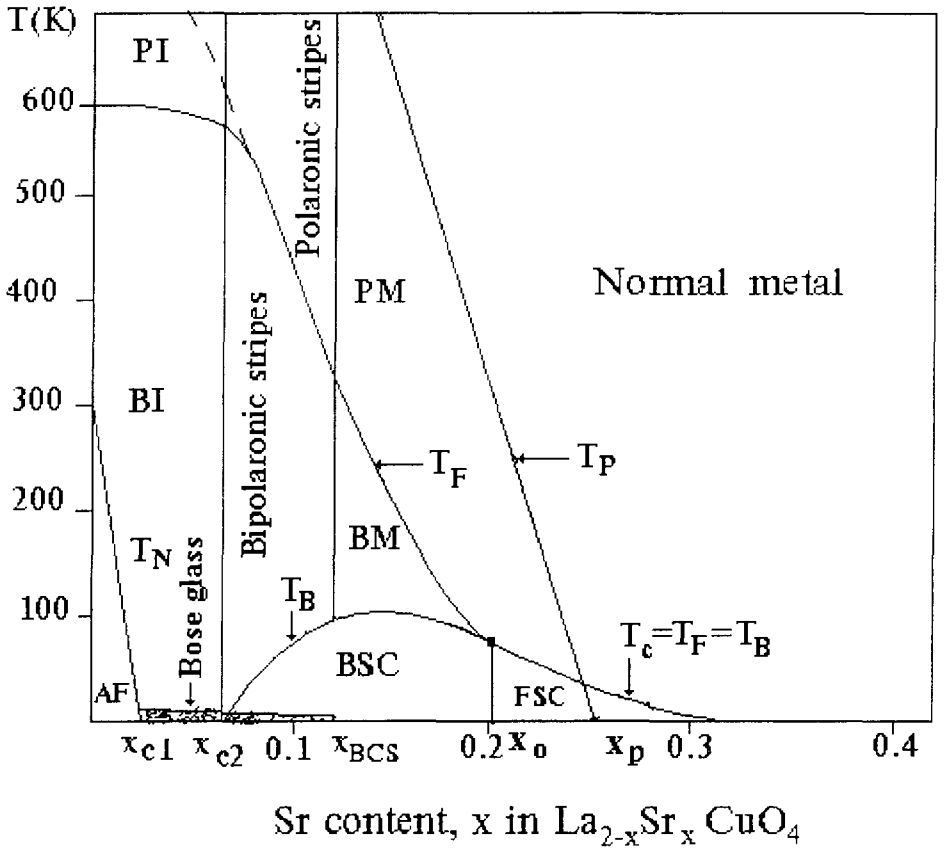
T(K)
600
500
400
300
200
100
PI
BI
PM
BM
BSC
FSC
AF
Bose glass
Bipolaronic stripes
Polaronic stripes
Normal metal
T_N
T_B
T_F
T_P
$T_c=T_F=T_B$
x_{c1}
x_{c2}
0.1
x_{BCS}
0.2
x_o
x_p
0.3
0.4
Sr content, x in $La_{2-x}Sr_x CuO_4$

Fig. 10b